

Infinite variety of thermodynamic speed limits with general activities

Ryuna Nagayama,^{1,*} Kohei Yoshimura,¹ and Sosuke Ito^{1,2}

¹*Department of Physics, The University of Tokyo, 7-3-1 Hongo, Bunkyo-ku, Tokyo 113-0033, Japan*

²*Universal Biology Institute, The University of Tokyo, 7-3-1 Hongo, Bunkyo-ku, Tokyo 113-0033, Japan*

Activity, which represents the kinetic property of dynamics, plays a central role in obtaining thermodynamic speed limits (TSLs). In this paper, we discuss a unified framework that provides the existing TSLs based on different activities such as dynamical activity and dynamical state mobility. We also derive an infinite variety of TSLs for Markov jump processes and deterministic chemical reaction networks by using different activities defined by the generalized means. The lower bound on the entropy production given by each TSL provides the minimum dissipation achievable by a conservative force. We numerically and analytically discuss the tightness of the lower bounds on the EPR in the various TSLs.

I. INTRODUCTION

One of the fundamental aims of nonequilibrium thermodynamics is to discover the laws governing dissipation, specifically the entropy production (EP) or its rate, the entropy production rate (EPR). The oldest and best known example is the second law of thermodynamics, which states that the EP is nonnegative. Recently, with the development of stochastic thermodynamics [1, 2], more refined laws applicable to Markov processes have been discovered. A prominent example is the thermodynamic speed limits (TSLs), which relate the speed of time evolution to the EP [3–6]. The TSLs have been shown to hold universally for various systems, including deterministic chemical reaction networks (CRNs) [7–10], deterministic reaction-diffusion systems [11], much like the second law of thermodynamics.

For Markov jump processes (MJPs), the dynamical activity, which determines the kinetic intensity of the system, plays a crucial role in the TSLs. A typical TSL for MJPs provides a lower bound on the EP by rescaling the square of the transition speed by the dynamical activity [4, 12]. To date, various efforts have been made to refine the relations between these three elements: the transition speed, the dynamical activity, and the EP. The variety of TSLs is based on the different approaches such as refining the functional forms that appear in TSLs [10, 13–16], measuring the speed with the 1-Wasserstein distance and the 2-Wasserstein distance from optimal transport theory [17–20] instead of the simple total variation distance [8, 11, 16, 21, 22], and using the Hatano-Sasa excess EP [23] or other generalizations of the excess EP, which is the portion of the EP that inherently affects the time evolution, instead of the total EP [4, 8, 10, 24].

For the TSLs based on the Wasserstein distances, alternative quantities are used instead of the dynamical activity to measure the kinetic intensity of the system: the dynamical state mobility [22] and the edgewise Onsager coefficient [8]. The difference between the dynamical activity and these alternative quantities can be understood in terms of means: the dynamical activity is twice the sum of the arithmetic mean of the forward and reverse jump rates for all transitions, whereas the dynamical state mobility is the sum of the logarithmic mean of these

rates. The edgewise Onsager coefficient is also introduced as the logarithmic mean of these rates for each transition. This mean perspective suggests that it is possible to derive distinct TSLs by altering the mean used to measure the kinetic intensity.

Indeed, in nonequilibrium thermodynamics for MJPs and CRNs, some activities have been developed based on various means different from the arithmetic and logarithmic means. For example, the geometric mean of bidirectional fluxes has been found in macroscopic fluctuation theory [12, 25–28]. This activity based on the geometric mean provides a lower bound of the EPR [29] and helps to decompose the EPR [30, 31]. Furthermore, activities based on more general means have been proposed to handle relaxation toward equilibrium mathematically [32]. However, it remains unclear whether these general activities can similarly lead to the derivation of the TSLs as those based on the arithmetic and logarithmic means.

In this paper, we derive an infinite variety of TSLs for MJPs and deterministic CRNs using general activities. We also use the 1-Wasserstein distance and its extension to CRNs [10, 11] to measure the speed of the time evolution. Our TSLs encompass previously established forms [21, 22]. We prove that a broad class of means, such as the Stolarsky mean containing infinitely many types of means [33–35], can be used as an activity. Because we can derive different TSLs for each choice of means, we obtain an infinite variety of TSLs. In nonstationary states, we numerically confirm that the tightness of the lower bounds on the EPR can vary in these different TSLs and that there is no apparent hierarchy for the tightness of the lower bounds in general. We show analytically that a hierarchy exists for the two specific means, i.e., maximum and minimum, and that a hierarchy also exists in the low-speed regime. We also numerically compare the proposed TSLs with the existing TSLs based on the 2-Wasserstein distance as lower bounds on the excess EPR [8, 10, 11]. In contrast to the EPR, we numerically confirm that the TSL for the excess EPR does not hold for some choice of mean.

We also reveal that each TSL yields minimum dissipation under different conditions depending on the mean employed as the activity. This unifies the two previously proposed approaches, one based on the arithmetic mean [21] and the other on the logarithmic mean [22]. We show that a conservative force and a time-independent current can achieve this mini-

* ryuna.nagayama@ubi.s.u-tokyo.ac.jp

imum dissipation, regardless of the mean used as the activity. For MJPs, whether a conservative force achieves minimum dissipation depends on the conditions for the minimization [8, 21, 22, 36, 37]. Our results provide a general class of conditions under which a conservative force can achieve minimum dissipation.

II. DYNAMICS AND THERMODYNAMICS ON NETWORKS AND CHEMICAL REACTION NETWORKS

In this study, we consider Markov jump processes (MJPs) and deterministic chemical reaction networks (CRNs). Based on the mathematical analogy [8, 38, 39], we can treat these different systems in the same way as shown below.

A. Dynamics

1. Markov jump process

Firstly, we consider a stochastic system consisting of N_S microstates without odd variables, which is described by an MJP. We index the microstates by $\alpha \in \mathcal{S}$, where \mathcal{S} denotes the index set of the microstates $\{1, 2, \dots, N_S\}$. We assume that the system is coupled with N_R heat reservoirs. We also define the index set of the thermodynamic reservoirs as $\mathcal{R} := \{1, 2, \dots, N_R\}$ and index the reservoirs by $\nu \in \mathcal{R}$.

We let the column vector $x(t) = (x_1(t), x_2(t), \dots, x_{N_S}(t))^T$ denote the probability distribution on the microstates at time t . We assume that the probability distribution satisfies $x_\alpha(t) > 0$ for all $\alpha \in \mathcal{S}$ and $\sum_{\alpha \in \mathcal{S}} x_\alpha(t) = 1$.

The probability distribution $x(t)$ evolves according to the following linear master equation,

$$d_t x_\alpha(t) = \sum_{\nu \in \mathcal{R}} \sum_{\beta \in \mathcal{S}} R_{\alpha\beta}^{(\nu)}(t) x_\beta(t), \quad (1)$$

where d_t denotes the time derivative d/dt , and $R_{\alpha\beta}^{(\nu)}(t)$ is the transition rate from microstate β to microstate α induced by reservoir ν at time t . We will omit the argument t if we do not focus on the time dependence. We make the following four assumptions on the transition rates: (i) $R_{\alpha\beta}^{(\nu)}$ is nonnegative if $\alpha \neq \beta$, (ii) $R_{\alpha\beta}^{(\nu)}$ is positive if and only if $R_{\beta\alpha}^{(\nu)}$ is positive, (iii) $R_{\alpha\beta}^{(\nu)}$ is always positive if it is positive at the initial time, and (iv) $R_{\alpha\alpha}^{(\nu)}$ satisfies $R_{\alpha\alpha}^{(\nu)} = -\sum_{\beta \in \mathcal{S} \setminus \{\alpha\}} R_{\beta\alpha}^{(\nu)} \leq 0$ for all $\alpha \in \mathcal{S}$ and $\nu \in \mathcal{R}$. Assumption (iv) ensures the conservation of probability, that is, $d_t \sum_{\alpha \in \mathcal{S}} x_\alpha = 0$.

To simplify the notation, we introduce the *directed edges* corresponding to the transitions as

$$(\beta \rightarrow \alpha; \nu), \quad (2)$$

for $\alpha, \beta \in \mathcal{S}$ and $\nu \in \mathcal{R}$ that satisfy $\alpha > \beta$ and $R_{\alpha\beta}^{(\nu)} > 0$. Due to assumption (iii) for the transition rates, we can define the directed edges independently of time. We refer to β, α ,

and ν as the start point, the target point, and the corresponding reservoir of the directed edge ($\beta \rightarrow \alpha; \nu$). We define the index set of the directed edges as $\mathcal{E} := \{1, 2, \dots, N_E\}$ with the number of the directed edges N_E . We index the directed edges by $e \in \mathcal{E}$. We also let $s(e)$, $t(e)$, and $r(e)$ denote the start point, the target point, and the corresponding reservoir of edge e , respectively. This enables us to represent edge e as $(s(e) \rightarrow t(e); r(e))$.

Using the directed edges, we define the forward and reverse fluxes on edge $e \in \mathcal{E}$ as

$$\begin{aligned} J_e^+(x, t) &:= R_{t(e)s(e)}^{(r(e))}(t) x_{s(e)}(t), \\ J_e^-(x, t) &:= R_{s(e)t(e)}^{(r(e))}(t) x_{t(e)}(t). \end{aligned} \quad (3)$$

Here, $J_e^+(x; t)dt$ gives the expected frequency of jump e in a short time interval dt , while $J_e^-(x; t)dt$ amounts to that of the inverse jump, which can be expressed as $(t(e) \rightarrow s(e); r(e))$. Note that all forward and reverse fluxes are positive due to the assumptions on the probability distributions and the transition rates. The forward and reverse fluxes let us define the (net) current along edge e as

$$J_e(x, t) := J_e^+(x, t) - J_e^-(x, t). \quad (4)$$

We also introduce the column vectors of the fluxes and the currents as $J^\pm(x, t) := (J_1^\pm(x, t), J_2^\pm(x, t), \dots, J_{N_E}^\pm(x, t))^T$ and $J(x, t) := (J_1(x, t), J_2(x, t), \dots, J_{N_E}(x, t))^T$. In the following, we will omit the arguments x and t to write $J(x)$, $J(t)$, or J , if we do not focus on the corresponding dependencies.

We can consider a directed graph with \mathcal{S} as the set of vertices and \mathcal{E} as the set of directed edges. This graph is characterized by an $N_E \times N_S$ matrix ∇ , whose element is defined as

$$\nabla_{e\alpha} := \delta_{\alpha t(e)} - \delta_{\alpha s(e)}. \quad (5)$$

for $e \in \mathcal{E}$ and $\alpha \in \mathcal{S}$. We refer to this matrix as the *gradient matrix* because it acts as the gradient operator. The transpose of the gradient matrix ∇^T can be interpreted as the negative divergence operator. For example, we can rewrite the linear master equation (1) as the following form:

$$d_t x = \nabla^T J = \nabla^T (J^+ - J^-). \quad (6)$$

If we regard ∇^T as the negative divergence, we can interpret this equation as a discrete continuity equation. We also note that the matrix ∇^T is often called the *incidence matrix* of the directed graph [40].

2. Chemical reaction network

Here, we use the same symbols as those used in the case of the MJP to indicate quantities in the CRN that play common roles.

We consider a CRN consisting of N_S internal species and N_E reversible reactions [41] at homogeneous temperature. We ignore external species that are exchanged with the outside of

the system since they do not affect our results. We let \mathcal{S} and \mathcal{E} denote the index sets of the internal species $\{1, \dots, N_S\}$ and the reversible reactions $\{1, \dots, N_E\}$, respectively. We also let X_α denote species $\alpha \in \mathcal{S}$.

The CRN is characterized by the number of molecules of species α consumed (produced) through reaction e , denoted by $n_{\alpha e}^+$ ($n_{\alpha e}^-$). Letting X_α denote species $\alpha \in \mathcal{S}$, reaction e is given by



Using $n_{\alpha e}^\pm$, we define the $N_E \times N_S$ *gradient matrix* of this CRN ∇ as

$$\nabla_{e\alpha} := n_{\alpha e}^- - n_{\alpha e}^+, \quad (8)$$

for $e \in \mathcal{E}$ and $\alpha \in \mathcal{S}$. The element $\nabla_{e\alpha}$ represents the net increase of the molecules of X_α through reaction e . The transpose of the gradient matrix ∇^\top is known as the stoichiometric matrix. As in the case of the MJP, the gradient matrix and its transpose act as the gradient operator and the negative divergence operator, respectively.

We represent the concentration distribution at time t by the column vector $x(t) = (x_1(t), x_2(t), \dots, x_{N_S}(t))^\top$. Here, $x_\alpha(t)$ represents the concentration of X_α at time t . We assume that $x_\alpha(t)$ is positive for all $\alpha \in \mathcal{S}$. In contrast to the case of the MJP, the distribution x does not necessarily satisfy $\sum_{\alpha \in \mathcal{S}} x_\alpha(t) = 1$, since the total concentration possibly changes through reactions.

The time evolution of the concentration distribution $x(t)$ is given by the rate equation. Using the stoichiometric matrix instead of the incidence matrix, the rate equation is represented by the continuity equation in Eq. (6). In this case, the net current $J_e(x, t)$ indicates the net reaction rate of reaction e . Since we consider reversible reactions, we assume that the net current $J_e(x, t)$ is given by the difference of the forward and reverse fluxes $J_e^\pm(x, t)$ as $J_e(x, t) = J_e^+(x, t) - J_e^-(x, t)$. The fluxes describe the unidirectional reaction rates of the forward and reverse reactions. Here, we also assume that all fluxes are positive $J_e^\pm(x, t) > 0$. In general, these fluxes $J_e^\pm(x, t)$ depend on the concentration distribution. For example, assuming the mass action kinetics, the forward and reverse fluxes are given by $J_e^\pm(x, t) := \kappa_e^\pm(t) \prod_{\alpha \in \mathcal{S}} [x_\alpha(t)]^{n_{\alpha e}^\pm}$ with the reaction rate constant $\kappa_e^\pm(t)$.

B. Thermodynamics

1. Steady state and equilibrium state

Before considering thermodynamic quantities, we introduce the concept of steady state and equilibrium state. In the following, we use 0 to indicate a column vector of dimension N_S or N_E with all components equal to zero.

The system is said to be in a steady state when its time evolution vanishes, i.e., when $d_t x = 0$ holds. Due to the continuity equation (6), the current J satisfies $\nabla^\top J = 0$ in a steady state. The system is also said to be in an equilibrium

state (or simply in equilibrium) when all currents vanish, i.e., when $J = 0$ holds. The system is in a steady state if it is in equilibrium, since $J = 0$ immediately yields $\nabla^\top J = 0$. We also refer to a steady state that is not an equilibrium state as a nonequilibrium steady state.

We also introduce the *detailed balance condition*, which guarantees the existence of an equilibrium state. If there exists a distribution $x^{\text{eq}}(t)$ that satisfies $J(x^{\text{eq}}(t), t) = 0$, the system is said to satisfy the detailed balance condition at time t . Here, $x^{\text{eq}}(t)$ indicates the equilibrium state at time t .

2. Thermodynamic force and entropy production rate

For the MJP and the CRN, we can introduce the thermodynamic force and the EPR in the same manner. In the following, we set the Boltzmann constant to one if we consider the MJP, and we take the gas constant as one if we consider the CRN.

We formally define the thermodynamic force for edge (reaction) e as

$$F_e(x, t) = \ln \frac{J_e^+(x, t)}{J_e^-(x, t)}. \quad (9)$$

We also simply refer to F_e as the force for edge (reaction) e . We also introduce the column vector of the forces as $F(x, t) := (F_1(x, t), F_2(x, t), \dots, F_{N_E}(x, t))^\top$. As in the case of the currents and fluxes, we will omit the arguments. We assume that the system satisfies the *local detailed balance* [42–44]. In the case of the MJP, this assumption enables us to interpret F_e as the increase of thermodynamic entropy of the system and the thermodynamic reservoirs through the transition on edge e . In the case of the CRN, this assumption enables us to interpret F_e as the increase of thermodynamic entropy of the solution and its environment (e.g., particle reservoir of the external species) through reaction e .

Using the forces, we define the EPR as

$$\sigma := \sum_{e \in \mathcal{E}} J_e F_e. \quad (10)$$

We can immediately obtain the second law of thermodynamics $\sigma \geq 0$, since the signs of J_e and F_e match for all $e \in \mathcal{E}$. Taking time integral of the EPR leads to the EP in the finite time duration $[0, \tau]$ as

$$\Sigma_\tau := \int_0^\tau dt \sigma. \quad (11)$$

The definition of F_e (9) and the relation $J_e = J_e^+ - J_e^-$ allow us to rewrite the EPR in Eq. (10) as [45]

$$\sigma = D_{\text{KL}}(J^+ \| J^-) + D_{\text{KL}}(J^- \| J^+). \quad (12)$$

Here, the Kullback–Leibler (KL) divergence between two N_E -dimensional vectors with positive elements, K and K' , is defined as

$$D_{\text{KL}}(K \| K') := \sum_{e \in \mathcal{E}} \left(K_e \ln \frac{K_e}{K'_e} - K_e + K'_e \right). \quad (13)$$

The KL divergence $D_{\text{KL}}(K\|K')$ becomes zero only when $K = K'$ holds. Due to this fact, equation (12) implies that the EPR becomes zero only when $J^+ = J^-$ holds, i.e., the system is in equilibrium. Thus, the EPR measures the irreversibility of the system, that is, the degree of nonequilibrium.

3. Conservativeness

We introduce the *conservativeness* of the forces, which is closely related to the detailed balance condition. If there exists a potential $\psi(t) = (\psi_1(t), \psi_2(t), \dots, \psi_{N_S}(t))^T$ that satisfies

$$F(t) = -\nabla\psi(t), \quad (14)$$

the forces are said to be conservative at time t . If we consider the MJP or the CRN with mass action kinetics, we can prove the equivalence of the following two statements: (i) the system satisfies the detailed balance condition at time t , and (ii) the forces are conservative at time t [46] (see Appendix A for the proof).

III. MEANS OF FORWARD AND REVERSE FLUXES AS ACTIVITIES

In stochastic thermodynamics, some means of forward and reverse fluxes are used to quantify the kinetic activity of MJPs. For example, the arithmetic mean, the geometric mean, and the logarithmic mean are used to define the dynamical activity [4, 12], the frenetic activity [29], and the dynamical state mobility [22] (or the edgewise Onsager coefficient [8]), respectively. Even in CRNs, the means of forward and reverse fluxes measure the intensity of reaction. In the following, we let $\mathbb{R}_{\geq 0}$ denote the set of all nonnegative real numbers.

A. Homogeneous symmetric mean

A bivariate function $m : \mathbb{R}_{\geq 0} \times \mathbb{R}_{\geq 0} \rightarrow \mathbb{R}_{\geq 0}$ is a *homogeneous symmetric mean* if $m(a, b)$ satisfies the following three properties for all $a, b \geq 0$: (i) upper and lower bounded as $\min(a, b) \leq m(a, b) \leq \max(a, b)$, (ii) symmetry ($m(a, b) = m(b, a)$), and (iii) homogeneity ($m(\lambda a, \lambda b) = \lambda m(a, b)$ for all $\lambda \geq 0$). We introduce some typical examples of homogeneous symmetric means in TABLE I. All the means that have been used as activities are homogeneous symmetric mean. In the following, we use the term *mean* to refer to homogeneous symmetric mean.

The symmetry and the homogeneity let us characterize m as

$$m(a, b) = b f_m\left(\frac{a}{b}\right), \quad (15)$$

with the representing function $f_m(r) := m(r, 1) = m(1, r)$ ($r \geq 0$) [47, 48]. Reflecting the symmetry and homogeneity of m , its representing function f_m satisfies the relation

$$f_m(r) = m(r, 1) = r m\left(1, \frac{1}{r}\right) = r f_m\left(\frac{1}{r}\right). \quad (16)$$

If $f_m(r)$ is differentiable, we also obtain

$$f_m(r) - r f'_m(r) = f'_m\left(\frac{1}{r}\right), \quad (17)$$

by taking r -derivative of the both sides in Eq. (16).

The representing function $f_m(r)$ also characterizes the hierarchy of means. We define a homogeneous symmetric mean m_1 to be smaller than another m_2 if $m_1(a, b) \leq m_2(a, b)$ holds for all $a, b \geq 0$, which we simply write $m_1 \leq m_2$. The representing function simplifies this condition into

$$\forall r \geq 0, f_{m_1}(r) \leq f_{m_2}(r). \quad (18)$$

We note that the typical means in TABLE I are listed in ascending order in terms of this inequality between means.

Several families of means enable us to treat many means in a stroke. For example, the Stolarsky mean [33–35] includes the means in TABLE I except the contraharmonic mean. The Stolarsky mean is defined for any $(p, q) \in \mathbb{R}^2$ as

$$S_{p,q}(a, b) := \begin{cases} \left[\frac{q(a^p - b^p)}{p(a^q - b^q)} \right]^{\frac{1}{p-q}} & (pq(p-q) \neq 0, a \neq b) \\ \left[\frac{a^p - b^p}{p(\ln a - \ln b)} \right]^{\frac{1}{p}} & (p \neq 0, q = 0, a \neq b) \\ \left[\frac{a^q - b^q}{q(\ln a - \ln b)} \right]^{\frac{1}{q}} & (p = 0, q \neq 0, a \neq b) \\ e^{-\frac{1}{p}} \left(\frac{a^{a^p}}{b^{b^p}} \right)^{\frac{1}{a^p - b^p}} & (p = q \neq 0, a \neq b) \\ \sqrt{ab} & (p = q = 0, a \neq b) \\ a & (a = b) \end{cases}. \quad (19)$$

We may regard the Stolarsky mean as one of the most general families of homogeneous symmetric means. This is because the Stolarsky mean includes some well-known families of homogeneous symmetric means parametrized by a real value. For example, taking $p = 2q$, we can reduce the Stolarsky mean to the Hölder mean [49] as,

$$S_{2q,q}(a, b) := \left(\frac{a^q + b^q}{2} \right)^{\frac{1}{q}}. \quad (20)$$

This family of means is also called the power mean. The means in TABLE I except the contraharmonic mean and the logarithmic mean are included in the Hölder mean. Taking $q = 1$, we can also reduce the Stolarsky mean to the mean introduced by Galvani [50] as

$$S_{p,1}(a, b) := \begin{cases} \left(\frac{a^p - b^p}{p(a - b)} \right)^{\frac{1}{p-1}} & (a \neq b) \\ a & (a = b) \end{cases}. \quad (21)$$

Note that some references refer to this family of means as the Stolarsky mean instead of Eq. (19). The means in TABLE I except the contraharmonic mean and the harmonic mean are included in this family.

TABLE I. Typical homogeneous symmetric means. Here the value of $L(a, a)$ is defined as a . The means are listed in order of decreasing.

Name	Concrete form
Minimum	$\min(a, b)$
Harmonic mean	$H(a, b) := \frac{2ab}{a+b}$
Geometric mean	$G(a, b) := \sqrt{ab}$
Logarithmic mean	$L(a, b) := \frac{a-b}{\ln a - \ln b}$
Arithmetic mean	$A(a, b) := \frac{a+b}{2}$
Contraharmonic mean	$C(a, b) := \frac{a^2 + b^2}{a+b}$
Maximum	$\max(a, b)$

B. General activity

We define the edgewise activity on edge e with a homogeneous symmetric mean m as

$$\mu_{m,e} := m(J_e^+, J_e^-). \quad (22)$$

In this definition, the average of the forward and reverse fluxes on edge e is measured with the mean m . We also define the activity measured with m as

$$\mu_m := \sum_{e \in \mathcal{E}} \mu_{m,e}. \quad (23)$$

This general activity turns into the well-known special cases as follows: the dynamical activity $\sum_{e \in \mathcal{E}} (J_e^+ + J_e^-)$ is given by $2\mu_A$, and the dynamical state mobility $\sum_{e \in \mathcal{E}} (J_e^+ - J_e^-) / (\ln J_e^+ - \ln J_e^-)$ is given by μ_L . Here, $A(a, b)$ and $L(a, b)$ corresponding to μ_A and μ_L are the arithmetic mean and the logarithmic mean introduced in TABLE I, respectively.

We can regard the general activity (23) as the total intensity of all jumps or reactions. Using different m corresponds to changing how to take the average of the forward and reverse rates. If we consider the continuum limit of MJPs, the general activity corresponds to the diffusion coefficient regardless of the choice of m (see Appendix B for details).

If the system is in a steady state, we can relate the activity to the time scale. In this case, the dynamical activity $2\mu_A$ indicates the total number of jumps or reactions per unit time in the steady state. Thus, we can define the time required for a single jump or reaction to occur as $\mathcal{T}_0 := (2\mu_A)^{-1}$. If we use m such that $m \leq A$, the general activity μ_m provides an upper bound of \mathcal{T}_0 as $\mathcal{T}_0 \leq (2\mu_m)^{-1}$. Conversely, if we use $m \geq A$, μ_m provides a lower bound as $\mathcal{T}_0 \geq (2\mu_m)^{-1}$.

C. Physical conditions on means

In the following, we only use homogeneous symmetric means whose representing function $f_m(r)$ is second-order differentiable at $r > 1$. We also impose the following two conditions on $f_m(r)$:

$$\forall r > 1, f_m'(r) + f_m'\left(\frac{1}{r}\right) > 0, \quad (24)$$

and

$$\forall r > 1, f_m''(r) \geq -\frac{r+1}{r(r-1)^2} \left[f_m'(r) + f_m'\left(\frac{1}{r}\right) \right]. \quad (25)$$

These two conditions are essential to obtain TSLs. While seemingly complex, these conditions are physically meaningful. We reveal the physical interpretation of each condition in the following two sections and Appendix C. Furthermore, these conditions are satisfied by broad means. For example, we can verify that the Stolarsky mean (19) satisfies these conditions (see Appendix D 1 for the proof). We can also verify that the contraharmonic mean, not included in the Stolarsky mean, satisfies the conditions (see Appendix D 2 for the proof). Thus, all of the typical means in TABLE I satisfy the conditions.

1. One by one relation between current and force induced by general activity

To reveal the meaning of the first condition (24), we introduce the fact that the activity enables us to relate the current and force. We can express J_e as a function of F_e with the activity $\mu_{m,e}$ as

$$J_e = \mu_{m,e} \Psi_m(F_e), \quad (26)$$

where $\Psi_m(u)$ is defined as

$$\Psi_m(u) := \frac{e^u - 1}{f_m(e^u)}. \quad (27)$$

This relation (26) is derived as follows: Using $J_e^+ / J_e^- = e^{F_e}$, we can represent J_e and $\mu_{m,e}$ with J_e^- and F_e as $J_e = J_e^- (e^{F_e} - 1)$ and $\mu_{m,e} = J_e^- f_m(J_e^+ / J_e^-) = J_e^- f_m(e^{F_e})$. Eliminating J_e^- from these two equations and using the definition of Ψ_m (27), we obtain the relation (26). We remark that the function Ψ_m is odd, which is verified by using the relation (16) as

$$\Psi_m(-u) = \frac{e^{-u} - 1}{f_m(e^{-u})} = \frac{e^{-u} - 1}{e^{-u} f_m(e^u)} = -\Psi_m(u). \quad (28)$$

Due to this oddness, the relation (26) connects $-F_e$ to $-J_e$ when it connects F_e to J_e . In particular, the relation links the force at the equilibrium $F_e = 0$ to the current at the equilibrium $J_e = 0$.

Physically, the condition (24) yields the inverse version of Eq. (26): we can express F_e as a function of J_e as

$$F_e = \Psi_m^{-1} \left(\frac{J_e}{\mu_{m,e}} \right). \quad (29)$$

Here, the existence of the inverse function Ψ_m^{-1} is verified by the fact that the condition (24) is equivalent to the monotonically increasingness of Ψ_m (see also Appendix C 1 for details). The inverse function Ψ_m^{-1} is odd and monotonically increasing since Ψ_m is so. In particular, due to the oddness, $-J_e$ is mapped to $-F_e$ in relation (26) when J_e mapped to F_e .

We now clarify the domain of the function Ψ_m^{-1} . While Ψ_m is defined over the entire set of real numbers, the domain of Ψ_m^{-1} is restricted to the range of Ψ_m . Specifically, $\Psi_m^{-1}(\omega)$ is defined only for ω satisfying $-\Psi_m(\infty) \leq \omega \leq \Psi_m(\infty)$ because $\Psi_m(u)$ is a monotonically increasing function and $\Psi_m(-u) = -\Psi_m(u)$. Here, we let $\Psi_m(\infty)$ denote the (possibly infinite) limit $\lim_{u \rightarrow \infty} \Psi_m(u)$. We note that Eq. (26) allows $J_e/\mu_{m,e}$ be included in the domain of Ψ_m^{-1} for all $e \in \mathcal{E}$.

We remark that the relations in Eq. (26) and Eq. (29) let the current and the force be mutually conjugate variables in terms of the Legendre duality. This duality is investigated and used to study the gradient structure of MJPs and CRNs [8, 18, 22, 25–27, 29, 30, 32, 51–53] (see also Appendix E for details). In particular, the duality with a general homogeneous symmetric mean has been discussed in Ref. [32]. However, they mainly focus on means whose representing function is concave for their mathematical purpose.

2. Monotonicity of entropy production rate

To reveal the meaning of the second condition (25), we rewrite the EPR using the relation in Eq. (29) as

$$\sigma = \sum_{e \in \mathcal{E}} J_e \Psi_m^{-1} \left(\frac{J_e}{\mu_{m,e}} \right). \quad (30)$$

Since the right-hand side can be rewritten as $\sum_{e \in \mathcal{E}} \mu_{m,e} (J_e/\mu_{m,e}) \Psi_m^{-1}(J_e/\mu_{m,e})$, the new representation (30) is characterized by a function $w \Psi_m^{-1}(w)$. We note that this function is even and monotonically increasing on $w > 0$ due to the oddness and monotonicity of Ψ_m^{-1} .

Under the first condition (24), the second condition (25) is equivalent to the convexity of $w \Psi_m^{-1}(w)$ (see also Appendix C 2 for details). This convexity implies that the EPR monotonically decreases by coarse-graining two edges e_1 and e_2 into one edge e_0 in the following way: The quantity on the coarse-grained edge is given by the sum of the quantities on the original edges as $J_{e_0} = J_{e_1} + J_{e_2}$ and $\mu_{m,e_0} = \mu_{m,e_1} + \mu_{m,e_2}$. Indeed, this monotonicity of the EPR is obtained by the convexity of $w \Psi_m^{-1}(w)$ as follows:

$$\begin{aligned} & J_{e_1} \Psi_m^{-1} \left(\frac{J_{e_1}}{\mu_{m,e_1}} \right) + J_{e_2} \Psi_m^{-1} \left(\frac{J_{e_2}}{\mu_{m,e_2}} \right) \\ &= \mu_{m,e_0} \sum_{i=1,2} \frac{\mu_{m,e_i}}{\mu_{m,e_0}} \left\{ \frac{J_{e_i}}{\mu_{m,e_i}} \Psi_m^{-1} \left(\frac{J_{e_i}}{\mu_{m,e_i}} \right) \right\} \\ &\geq J_{e_0} \Psi_m^{-1} \left(\frac{J_{e_0}}{\mu_{m,e_0}} \right). \end{aligned}$$

Here, $J_{e_0}/\mu_{m,e_0}$ is included in the domain of Ψ_m^{-1} , since

this quantity is the convex combination of $J_{e_1}/\mu_{m,e_1}$ and $J_{e_2}/\mu_{m,e_2}$.

IV. THERMODYNAMIC SPEED LIMITS WITH THE 1-WASSERSTEIN DISTANCE

A. Bounds for general currents

We here introduce a trade-off relation which is essential for the derivation of the TSLs. The trade-off relation provides a lower bound of the time average of the EPR $\langle \sigma \rangle_\tau$ by the speed of the time evolution of a general observable.

The monotonically decreasingness of the EPR discussed in Sec. III C 2 yields the trade-off relation between the dissipation and the intensity of a general current. The trade-off relation is represented as the following lower bound of $\langle \sigma \rangle_\tau$ with a general current $\mathcal{J}_c(t) := \sum_{e \in \mathcal{E}} c_e(t) J_e(t)$:

$$\langle \sigma \rangle_\tau \geq \frac{\langle |\mathcal{J}_c| \rangle_\tau}{|c|_\infty} \Psi_m^{-1} \left(\frac{\langle |\mathcal{J}_c| \rangle_\tau}{|c|_\infty \langle \mu_m \rangle_\tau} \right). \quad (31)$$

Here, we let $|c|_\infty$ denote $\max_{e \in \mathcal{E}, t \in [0, \tau]} |c_e(t)|$. We also define the time average as $\langle \bullet \rangle_\tau = (1/\tau) \int_0^\tau dt \bullet$. The lower bound in Eq. (31) is monotonically increasing with $\langle |\mathcal{J}_c| \rangle_\tau$ and monotonically decreasing with $\langle \mu_m \rangle_\tau$. Thus, this bound implies that a larger EP is required to realize a more intense current with lower activity.

This inequality (31) is derived by applying Jensen's inequality for the convex function $\omega \Psi_m^{-1}(\omega)$ (see Appendix F 1 for the proof). In Appendix F 2, we also discuss an application of the trade-off relation as a bound for statewise observables.

B. 1-Wasserstein distance and speed of the time evolution

We define the 1-Wasserstein distance between the two distributions x^A and x^B via the following minimization problem,

$$W_1(x^A, x^B) = \inf_U \sum_{e \in \mathcal{E}} |U_e|, \quad (32)$$

where the infimum is over all $U = (U_1, U_2, \dots, U_{N_E})^\top$ satisfying $x^B - x^A = \nabla^\top U$. In the case of the MJPs, it is well known as the Beckmann problem [20, 54], which is generalized to chemical systems in nonequilibrium thermodynamics [11]. Note that the condition on U lets us define the 1-Wasserstein distance between x^A and x^B only when $x^B - x^A$ belongs to the image of ∇^\top .

We remark that the Beckmann problem is the dual problem of another optimization problem, which is called the Kantorovich–Rubinstein duality [17, 20]. We also introduce this duality formula in Appendix G.

The 1-Wasserstein distance enables us to measure the speed of the time evolution as

$$v_1(t) := \lim_{\Delta t \rightarrow 0} \frac{W_1(x(t), x(t + \Delta t))}{\Delta t}. \quad (33)$$

TABLE II. The TSLs with typical means. We also show the concrete form of the edgewise activities and the functions $\Psi_m(u)$ and $\Psi_m^{-1}(\omega)$. Due to Eq. (39), we only show the forms of $\Psi_m(u)$ and $\Psi_m^{-1}(\omega)$ on $u \geq 0$ and $0 \leq \omega \leq \Psi_m(\infty)$, respectively

Mean	$\mu_{m,e}$	$\Psi_m(u)$ ($u \geq 0$)	$\Psi_m^{-1}(\omega)$ ($0 \leq \omega \leq \Psi_m(\infty)$)	TSL
Minimum	$\min(J_e^+, J_e^-)$	$e^u - 1$	$\ln(1 + \omega)$	$\langle \sigma \rangle_\tau \geq \langle v_1 \rangle_\tau \ln \left(1 + \frac{\langle v_1 \rangle_\tau}{\langle \mu_m \rangle_\tau} \right)$
Harmonic mean	$\frac{2J_e^+ J_e^-}{J_e^+ + J_e^-}$	$\sinh u$	$\sinh^{-1} \omega$	$\langle \sigma \rangle_\tau \geq \langle v_1 \rangle_\tau \sinh^{-1} \left(\frac{\langle v_1 \rangle_\tau}{\langle \mu_m \rangle_\tau} \right)$
Geometric mean	$\sqrt{J_e^+ J_e^-}$	$2 \sinh \frac{u}{2}$	$2 \sinh^{-1} \frac{\omega}{2}$	$\langle \sigma \rangle_\tau \geq 2 \langle v_1 \rangle_\tau \sinh^{-1} \left(\frac{\langle v_1 \rangle_\tau}{2 \langle \mu_m \rangle_\tau} \right)$
Logarithmic mean	$\frac{J_e^+ - J_e^-}{\ln J_e^+ - \ln J_e^-}$	u	ω	$\langle \sigma \rangle_\tau \geq \frac{\langle v_1 \rangle_\tau^2}{\langle \mu_m \rangle_\tau}$
Arithmetic mean	$\frac{J_e^+ + J_e^-}{2}$	$2 \tanh \frac{u}{2}$	$2 \tanh^{-1} \frac{\omega}{2}$	$\langle \sigma \rangle_\tau \geq 2 \langle v_1 \rangle_\tau \tanh^{-1} \left(\frac{\langle v_1 \rangle_\tau}{2 \langle \mu_m \rangle_\tau} \right)$
Contraharmonic mean	$\frac{(J_e^+)^2 + (J_e^-)^2}{J_e^+ + J_e^-}$	$\tanh u$	$\tanh^{-1} \omega$	$\langle \sigma \rangle_\tau \geq \langle v_1 \rangle_\tau \tanh^{-1} \left(\frac{\langle v_1 \rangle_\tau}{\langle \mu_m \rangle_\tau} \right)$
Maximum	$\max(J_e^+, J_e^-)$	$1 - e^{-u}$	$-\ln(1 - \omega)$	$\langle \sigma \rangle_\tau \geq -\langle v_1 \rangle_\tau \ln \left(1 - \frac{\langle v_1 \rangle_\tau}{\langle \mu_m \rangle_\tau} \right)$

The Beckmann problem (32) provides the upper bound of the speed,

$$v_1(t) \leq \sum_{e \in \mathcal{E}} |J_e(t)|. \quad (34)$$

This bound is obtained as follows. Since $x(t + \Delta t) - x(t) = \Delta t \nabla^\top J(t) + O(\Delta t^2)$ holds, $\Delta t J(t) + O(\Delta t^2)$ is a candidate of the optimization problem corresponding to $W_1(x(t), x(t + \Delta t))$. It immediately leads to $W_1(x(t), x(t + \Delta t)) \leq \Delta t \sum_{e \in \mathcal{E}} |J_e(t)| + O(\Delta t^2)$. Deviding both sides of this inequality by Δt and taking the limit $\Delta t \rightarrow 0$ conclude the desired bound (34).

C. Thermodynamic speed limits with the 1-Wasserstein distance

Using the speed measured with the 1-Wasserstein distance (33) and the general activity, we can obtain a series of TSLs,

$$\langle \sigma \rangle_\tau \geq \langle v_1 \rangle_\tau \Psi_m^{-1} \left(\frac{\langle v_1 \rangle_\tau}{\langle \mu_m \rangle_\tau} \right) \quad (35)$$

$$\geq \frac{W_1(x(0), x(\tau))}{\tau} \Psi_m^{-1} \left(\frac{W_1(x(0), x(\tau))}{\tau \langle \mu_m \rangle_\tau} \right). \quad (36)$$

The equation (35) is derived from the lower bound of the EP (31) and the inequality for the speed (34) as follows. Taking the coefficient c_e in the trade-off relation (31) as

$$c_e(t) := \begin{cases} 1 & (J_e(t) \geq 0) \\ -1 & (J_e(t) < 0) \end{cases}, \quad (37)$$

we obtain

$$\langle \sigma \rangle_\tau \geq \left\langle \sum_{e \in \mathcal{E}} |J_e| \right\rangle_\tau \Psi_m^{-1} \left(\frac{\langle \sum_{e \in \mathcal{E}} |J_e| \rangle_\tau}{\langle \mu_m \rangle_\tau} \right), \quad (38)$$

since $|c|_\infty = 1$. Combining this inequality and Eq. (34), we can obtain Eq. (35) because the function $\omega \Psi_m^{-1}(\omega)$ is monotonically increasing on $\omega \geq 0$. The inequality in Eq. (36) is also obtained by the triangle inequality of the 1-Wasserstein distance $\int_0^\tau dt v_1(t) \geq W_1(x(0), x(\tau))$. We also provide another proof with the Kantorovich–Rubinstein duality in Appendix H.

We note that the arguments of Ψ_m^{-1} appearing in Eqs. (35) and (36) are included in the nonnegative domain $0 \leq \omega \leq \Psi_m(\infty)$. This is because the following inequalities hold:

$$0 \leq \frac{W_1(x(0), x(\tau))}{\tau \langle \mu_m \rangle_\tau} \leq \frac{\langle v_1 \rangle_\tau}{\langle \mu_m \rangle_\tau} \leq \Psi_m(\infty). \quad (39)$$

Here, the first and the second inequalities follow from the nonnegativity and the triangle inequality of the 1-Wasserstein distance, respectively. The last one is obtained as

$$\frac{\langle v_1 \rangle_\tau}{\langle \mu_m \rangle_\tau} \leq \frac{\int_0^\tau dt \sum_{e \in \mathcal{E}} |J_e|}{\int_0^\tau dt \sum_{e \in \mathcal{E}} \mu_{m,e}} \leq \max_{e \in \mathcal{E}, t \in [0, \tau]} \frac{|J_e|}{\mu_{m,e}} \leq \Psi_m(\infty), \quad (40)$$

where we use Eq. (26), Eq. (34), the monotonically increasingness of Ψ_m , and the following inequality:

$$\begin{aligned} & \int_0^\tau dt \sum_{e \in \mathcal{E}} \mu_{m,e} \frac{|J_e|}{\mu_{m,e}} \\ & \leq \left(\int_0^\tau dt \sum_{e \in \mathcal{E}} \mu_{m,e} \right) \left(\max_{e \in \mathcal{E}, t \in [0, \tau]} \frac{|J_e|}{\mu_{m,e}} \right). \end{aligned} \quad (41)$$

Physically, the TSL (35) represent the trade-off relation between three elements, the dissipation, the speed of the time evolution, and the activity. Since the lower bound $\langle v_1 \rangle_\tau \Psi_m^{-1}(\langle v_1 \rangle_\tau / \langle \mu_m \rangle_\tau)$ increases with respect to $\langle v_1 \rangle_\tau$ and decreases with respect to $\langle \mu_m \rangle_\tau$, we need greater dissipation to evolve the system with faster speed or smaller activity.

Substituting various means satisfying the conditions in Eqs. (24) and (25) into the general forms in Eqs. (35) and (36), we can obtain an infinite variety of TSLs. For example, using the Stolarsky mean $S_{p,q}$ as m in Eqs. (35) and (36) provides TSLs for all pairs of real numbers (p, q) . In general, we need to compute the inverse function Ψ_m^{-1} numerically to verify the TSLs, since it does not have closed forms. However, the TSLs reduce to some simple forms for several means: All typical means in TABLE I let the TSLs be simple as shown in TABLE II. We remark that the TSL with the arithmetic mean

$$\langle \sigma \rangle_\tau \geq \frac{2W_1(x(0), x(\tau))}{\tau} \tanh^{-1} \left(\frac{W_1(x(0), x(\tau))}{2\tau \langle \mu_A \rangle_\tau} \right), \quad (42)$$

and the one with the logarithmic mean

$$\langle \sigma \rangle_\tau \geq \frac{W_1(x(0), x(\tau))^2}{\tau^2 \langle \mu_L \rangle_\tau}, \quad (43)$$

are the same as the ones in the previous studies [21, 22].

We can also rewrite the TSLs (35) and (36) into lower bounds of the transition time τ . To do so, we define the path length of the time series of x as $l_{1,\tau} := \int_0^\tau dt v_1$. Using the relations $\tau \langle v_1 \rangle_\tau = l_{1,\tau}$ and $\tau \langle \sigma \rangle_\tau = \Sigma_\tau$, we obtain

$$\begin{aligned} \tau &\geq \left[\frac{\langle \mu_m \rangle_\tau \Psi_m \left(\frac{\Sigma_\tau}{l_{1,\tau}} \right)}{l_{1,\tau}} \right]^{-1} \\ &\geq \left[\frac{\langle \mu_m \rangle_\tau}{W_1(x(0), x(\tau))} \Psi_m \left(\frac{\Sigma_\tau}{W_1(x(0), x(\tau))} \right) \right]^{-1}. \end{aligned} \quad (44)$$

We provide the derivation in Appendix I. We can regard the first lower bound in Eq. (44) as the minimum time required to evolve the system along the original path $\{x(t)\}_{t \in [0, \tau]}$. The second lower bound in Eq. (44) also provides the minimum time required to evolve the system from $x(0)$ to $x(\tau)$, where the path may be different from the original one. In both cases, we can reduce the minimum time by spending more dissipation or achieving greater activity. In contrast to the original form (35) and (36), we can obtain these lower bounds without calculating the inverse function Ψ_m^{-1} .

Historically, TSLs for MJPs are derived using a simpler distance, called the total variation distance, $d_{TV}(x^A, x^B) := \sum_{\alpha \in \mathcal{S}} |x_\alpha^B - x_\alpha^A|/2$ [4, 13]. This definition is applicable even in the case of CRNs. We can also verify that the total variation distance provides a lower bound of the 1-Wasserstein distance. Thus, the total variation distance leads to weaker TSLs (see also Appendix J for details).

D. Appearance of hierarchy in low-speed regimes

In general, a hierarchy of means $m_1 \leq m_2$ does not provide a hierarchy of the TSLs, that is an apparent inequal-

ity between the two lower bounds $\langle v_1 \rangle_\tau \Psi_{m_1}^{-1}(\langle v_1 \rangle_\tau / \langle \mu_{m_1} \rangle_\tau)$ and $\langle v_1 \rangle_\tau \Psi_{m_2}^{-1}(\langle v_1 \rangle_\tau / \langle \mu_{m_2} \rangle_\tau)$. Therefore, there is no definite choice of the mean, which provides the tightest bound in the TSLs. In general, we can only obtain the two inequalities $\langle \mu_{m_1} \rangle_\tau \leq \langle \mu_{m_2} \rangle_\tau$ and

$$\Psi_{m_1}^{-1}(\omega) \leq \Psi_{m_2}^{-1}(\omega), \quad (45)$$

for any $0 \leq \omega \leq \Psi_{m_2}(\infty)$ when $m_1 \leq m_2$. This is because μ_m is monotonically increasing in m , and Eq. (45) follows from the fact $\Psi_{m_1}(u) \geq \Psi_{m_2}(u)$ and the monotonically increasingness of Ψ_m . Here, $\Psi_{m_1}(u) \geq \Psi_{m_2}(u)$ is obtained from $f_{m_1}(r) \leq f_{m_2}(r)$. These two general inequalities do not provide an apparent inequality between the two lower bounds. In fact, we have found numerically that the tightness of the TSLs between two means can change over time as discussed later.

However, it may be possible to show the existence of a hierarchy between TSLs with two specific means. For example, we can show that the TSL with $\min(a, b)$ is always tighter than (or equivalent to) the TSL with $\max(a, b)$ as follows. Combining the relation $\mu_{\max, e} - \mu_{\min, e} = |J_e|$ and the inequality in Eq. (34), we obtain

$$\langle \mu_{\max} \rangle_\tau - \langle \mu_{\min} \rangle_\tau = \left\langle \sum_{e \in \mathcal{E}} |J_e| \right\rangle_\tau \geq \langle v_1 \rangle_\tau. \quad (46)$$

Using this inequality (46) and nonnegativities of $\langle \mu_{\min} \rangle_\tau$ and $\langle v_1 \rangle_\tau$, we can easily verify that the following inequality holds:

$$\left(1 - \frac{\langle v_1 \rangle_\tau}{\langle \mu_{\max} \rangle_\tau} \right)^{-1} \leq 1 + \frac{\langle v_1 \rangle_\tau}{\langle \mu_{\min} \rangle_\tau}. \quad (47)$$

By taking the logarithm of both sides of this inequality (47) and then multiplying both sides by $\langle v_1 \rangle_\tau$, we obtain the hierarchy between the TSLs with $\max(a, b)$ and $\min(a, b)$ as

$$-\langle v_1 \rangle_\tau \ln \left(1 - \frac{\langle v_1 \rangle_\tau}{\langle \mu_{\max} \rangle_\tau} \right) \leq \langle v_1 \rangle_\tau \ln \left(1 + \frac{\langle v_1 \rangle_\tau}{\langle \mu_{\min} \rangle_\tau} \right), \quad (48)$$

or equivalently

$$\langle v_1 \rangle_\tau \Psi_{\max}^{-1} \left(\frac{\langle v_1 \rangle_\tau}{\langle \mu_{\max} \rangle_\tau} \right) \leq \langle v_1 \rangle_\tau \Psi_{\min}^{-1} \left(\frac{\langle v_1 \rangle_\tau}{\langle \mu_{\min} \rangle_\tau} \right). \quad (49)$$

Moreover, we have a hierarchy of the TSLs if the state is close to a steady state: the smaller the mean, the tighter the bound. Close to the steady state, the speed decreases, while the activity remains finite. Thus, we can assume $\langle v_1 \rangle_\tau \ll \langle \mu_m \rangle_\tau$. This assumption allows us to expand $\Psi_m^{-1}(\langle v_1 \rangle_\tau / \langle \mu_m \rangle_\tau)$ in the TSL (35) using a Taylor series as

$$\Psi_m^{-1} \left(\frac{\langle v_1 \rangle_\tau}{\langle \mu_m \rangle_\tau} \right) = \frac{\langle v_1 \rangle_\tau}{\langle \mu_m \rangle_\tau} + O \left(\left(\frac{\langle v_1 \rangle_\tau}{\langle \mu_m \rangle_\tau} \right)^3 \right). \quad (50)$$

Here, we used $\Psi_m^{-1}(0) = 0$ and $(\Psi_m^{-1})'(0) = 1/\Psi_m'(0) = 1$. We note that the even-order terms of $\langle v_1 \rangle_\tau / \langle \mu_m \rangle_\tau$ vanish

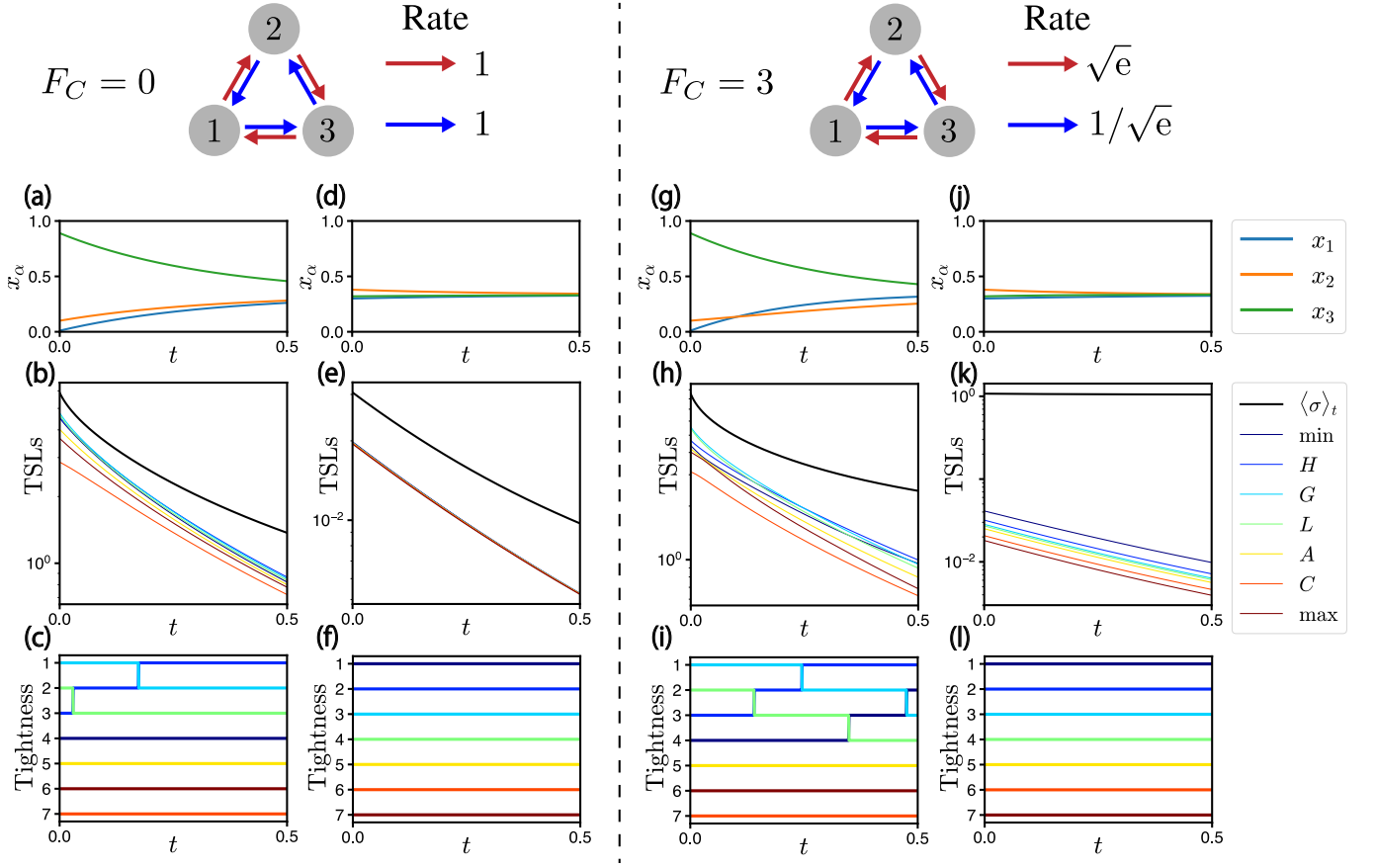


FIG. 1. The hierarchy of TSLs (35) in TABLE II. We compare the TSLs (35) in detailed balanced and driven systems near and far from steady state. The region to the left of the dashed line corresponds to the detailed balanced system ($F_C = 0$), while the region to the right corresponds to the driven system ($F_C = 3$). We also show the system used in this numerical calculation. The gray circles correspond to microstates. We take the transition rates for moving between microstates clockwise (red arrows) and counterclockwise (blue arrows) as $e^{F_C/6}$ and $e^{-F_C/6}$, respectively. (a) Time series of the probability distribution in case (I) ($F_C = 0$, $x(0) = (0.01, 0.1, 0.89)^\top$). (b) The TSLs in case (I). (c) The tightness of the TSLs in case (I). (d) Time series of the probability distribution in case (II) ($F_C = 0$, $x(0) = (0.3, 0.38, 0.32)^\top$). (e) The TSLs in case (II). Since the system is near equilibrium, all the TSLs provide almost the same lower bounds. (f) The tightness of the TSLs in case (II). The TSL becomes tighter with smaller means because the speed of the time evolution is slow. (g) Time series of the probability distribution in case (III) ($F_C = 3$, $x(0) = (0.01, 0.1, 0.89)^\top$). (h) The TSLs in case (III). (i) The tightness of the TSLs in case (III). (j) Time series of the probability distribution in case (IV) ($F_C = 3$, $x(0) = (0.3, 0.38, 0.32)^\top$). (k) The TSLs in case (IV). (l) The tightness of the TSLs in case (IV). Since the system is near the nonequilibrium steady state, the TSL with a smaller mean provides a tighter bound. In (b), (e), (h), and (k), the black line indicates $\langle \sigma \rangle_\tau$. The other lines indicate the lower bounds of $\langle \sigma \rangle_\tau$ provided by the TSLs in TABLE II (in the legend, we only indicate the means used as the activity). In (c), (f), (i), and (l), the smaller the number, the tighter the lower bound on the EPR. The colors of lines correspond to the mean used in the TSLs.

because $\Psi_m^{-1}(\omega)$ is an odd function. Due to this expansion, the TSL reduces to

$$\langle \sigma \rangle_\tau \geq \frac{\langle v_1 \rangle_\tau^2}{\langle \mu_m \rangle_\tau}. \quad (51)$$

This form implies that the TSL with a smaller mean becomes tighter.

In addition, the TSL (35) gives almost the same bound regardless of the mean used if the system is near equilibrium. In this situation, we can take a small constant ϵ_{eq} satisfying $|J_e| \leq \epsilon_{\text{eq}}$ for all $e \in \mathcal{E}$. This is because all currents vanish in equilibrium. Then, we can use the representation in Eq. (51), since the inequality for v_1 (34) yields $v_1 \leq \sum_{e \in \mathcal{E}} |J_e| \leq$

$N_E \epsilon_{\text{eq}}$. We can also obtain

$$\mu_{m,e} = m(J_e^+, J_e^-) = J_e^+ + O(\epsilon_{\text{eq}}) \quad (52)$$

because any homogeneous symmetric mean m is bounded as $\min(a, b) \leq m(a, b) \leq \max(a, b)$. Thus, the TSL (35) reduces to

$$\langle \sigma \rangle_\tau \geq \frac{\langle v_1 \rangle_\tau^2}{\langle \sum_{e \in \mathcal{E}} |J_e^+| \rangle_\tau}, \quad (53)$$

which is independent of m . Here, the hierarchy of the TSLs arises from the higher-order terms of ϵ_{eq} .

In Fig. 1, we numerically demonstrate the above facts using the MJP with three microstates $\mathcal{S} = \{1, 2, 3\}$ and one heat

reservoir $\mathcal{R} = \{1\}$. We set the transition rates as $R_{21}^{(1)} = R_{32}^{(1)} = R_{13}^{(1)} = e^{F_C/6}$ and $R_{12}^{(1)} = R_{23}^{(1)} = R_{31}^{(1)} = e^{-F_C/6}$. Here, F_C corresponds to the cycle affinity [2, 55]. The steady state is given by $x^{\text{st}} := (1/3, 1/3, 1/3)^\top$ regardless of F_C . This steady state becomes an equilibrium state only when F_C is zero. In the following calculations, we consider the following four cases: (I) far from equilibrium ($F_C = 0$, $x(0) = (0.01, 0.1, 0.89)^\top$), (II) near equilibrium ($F_C = 0$, $x(0) = (0.3, 0.38, 0.32)^\top$), (III) far from the nonequilibrium steady state ($F_C = 3$, $x(0) = (0.01, 0.1, 0.89)^\top$), and (IV) near the nonequilibrium steady state ($F_C = 3$, $x(0) = (0.3, 0.38, 0.32)^\top$).

First, we focus on the cases of $F_C = 0$, where the system relaxes to the equilibrium. In case (I), the distribution evolves fast as shown in Fig. 1(a). Since the speed of the time evolution is not small, a smaller mean does not necessarily provide a tighter bound as shown in Fig. 1(b) and (c). For example, the contraharmonic mean yields the weakest bound even though this mean is smaller than the maximum. The harmonic, geometric, and logarithmic means provide tighter bounds than the one based on the smallest mean, the minimum. Although the ordering of the bounds can vary depending on t as shown in Fig. 1(c), we can confirm the hierarchy between the TSLs based on min and max in Eq. (48). In contrast to case (I), the speed of the time evolution is slow in case (II) [Fig. 1(d)]. In case (II), the bounds take almost the same values as shown in Fig. 1(e), since the system is near equilibrium. We can see the hierarchy in Fig. 1(f): a smaller mean provides a tighter bound, since v_1 is slow.

Second, we focus on the cases of $F_C = 3$, where the system approaches the nonequilibrium steady state. Figure 1(g-i) shows the details of case (III). This case is similar to case (I) because the speed of the time evolution is not small. A smaller mean does not necessarily provide a tighter bound, and the ordering of the bounds can vary depending on t . The hierarchy between the TSLs based on min and max in Eq. (48) also holds as shown in Fig. 1(i). In case (IV), the speed of the time evolution is slow as in case (II) [Fig. 1(j)]. In this case, the bounds take different values as shown in Fig. 1(k). This is because the system is not near equilibrium. We can also see the hierarchy between TSLs in Fig. 1(l), since v_1 is slow.

E. Minimum dissipation and achievability of equality in TSLs

As in the special cases [21, 22], the lower bound of the dissipation in Eq. (36) provides a minimum dissipation formula. Under the optimal protocol that achieves the minimum dissipation, the both lower bounds in Eq. (36) coincide with $\langle \sigma \rangle_\tau$; in other words, the equalities in the TSLs are achieved.

We show these facts by considering a minimum dissipation required to evolve the state from $x(0)$ to $x(\tau)$ over time τ under some physically valid conditions. In the following, we regard the EP and the time average of the activity as functionals of

the fluxes as

$$\left\{ \begin{array}{l} \Sigma_\tau[J^+, J^-] := \int_0^\tau dt \sum_{e \in \mathcal{E}} (J_e^+ - J_e^-) \ln \frac{J_e^+}{J_e^-}, \\ \langle \mu_m \rangle_\tau[J^+, J^-] := \frac{1}{\tau} \int_0^\tau dt \sum_{e \in \mathcal{E}} m(J_e^+, J_e^-). \end{array} \right. \quad (54)$$

We consider the minimization problem $\inf_{J^+, J^-} \Sigma_\tau[J^+, J^-]$ under the following conditions: (i) the fluxes evolve the distribution from $x(0)$ to $x(\tau)$ as

$$x(\tau) - x(0) = \nabla^\top \int_0^\tau dt (J^+ - J^-), \quad (56)$$

(ii) the time average of the activity is bounded by a constant M_0 as

$$\langle \mu_m \rangle_\tau[J^+, J^-] \leq M_0, \quad (57)$$

(iii) if $J_e^+ = J_e^- = 0$ holds, we regard $(J_e^+ - J_e^-) \ln(J_e^+/J_e^-)$ as zero. Condition (iii) is physically valid since $J_e^+ = J_e^- = 0$ implies that jump does not occur on edge e for MJPs and reaction e does not proceed for CRNs. Then, the minimum dissipation is related to the 1-Wasserstein distance as

$$\begin{aligned} & \inf_{J^+, J^-} \Sigma_\tau[J^+, J^-] \\ &= W_1(x(0), x(\tau)) \Psi_m^{-1} \left(\frac{W_1(x(0), x(\tau))}{\tau M_0} \right). \end{aligned} \quad (58)$$

We remark that we can make the EP zero by allowing the activity to have an infinite value [21]. We impose condition (ii) to prevent such non-physical optimization. We provide the derivation of the minimum dissipation formula (58) in Appendix K.

As an optimizer of this minimization problem, we can take the fluxes $J^{+\star}$ and $J^{-\star}$ that satisfy the following properties: (a) The current generated by $J^{+\star}$ and $J^{-\star}$, i.e., $J^\star := J^{+\star} - J^{-\star}$, is independent of time. (b) There exists a potential $\tilde{\varphi}$ that satisfies

$$\ln \frac{J_e^{+\star}}{J_e^{-\star}} = -(\nabla \tilde{\varphi})_e, \quad (59)$$

for all e where $J_e^{\pm\star} \neq 0$. Property (a) determines the concrete form of the distribution evolved by the optimal current J^\star from $x(0)$, denoted by x^\star , as

$$x^\star(t) := \left(1 - \frac{t}{\tau}\right) x(0) + \frac{t}{\tau} x(\tau). \quad (60)$$

It is easily verified by solving $d_t x^\star = \nabla^\top J^\star$ with the initial condition $x^\star(0) = x(0)$. Property (b) implies that the force generated by $J^{\pm\star}$ can be regarded as a conservative force after removing the edges that satisfy $J_e^{\pm\star} = 0$. We note that this removal of edges does not affect the time evolution and dissipation. This conservativeness is based on the Kantorovich–Rubinstein duality. We provide further details of the optimizers $J^{+\star}$ and $J^{-\star}$ in Appendix K.

For special cases ($m = A, L$), previous studies show that the optimal force can be realized by a conservative force [21, 22]. Generally, whether a conservative force can achieve the minimum EP in MJPs depends on the conditions imposed on the minimization problem [8, 36, 37]. Our results show that under the constraint in Eq. (57), the minimum EP can always be achieved by a conservative force, regardless of which activity is used.

The minimum dissipation (58) ensures that the lower bound in Eq. (36) is achievable. Then the two lower bounds in Eqs. (35) and (36) coincide. Thus, the TSLs can be seen as achievable bounds. It is remarkable that in the optimal situation, the EPR also becomes time independent since the optimizer is, as discussed.

V. COMPARISON WITH EXCESS ENTROPY PRODUCTION RATES AND TSL FOR 2-WASSERSTEIN DISTANCE

The TSLs are inequalities about the speed of the time evolution. This fact implies that TSLs are related to the nonstationarity of the system. Therefore, some TSLs can be tightened by replacing the EPR with the excess EPR [56], which may be the nonstationary contribution of the EPR.

The definition of the excess EPR is not unique [23, 57]. A typical example is the Hatano–Sasa excess (or nonadiabatic) EPR [23, 58]. This method is based on the steady state, and applicable to limited systems: Markov processes and a special class of CRNs, which is called complex balanced CRNs [39]. To consider more general systems, the geometric excess/housekeeping decomposition for Langevin systems [59–61] has been extended based on different geometries: optimal transport theory [8], information geometry [10], and Hessian geometry [30]. Especially, the excess EPR based on optimal transport theory [8] is related to the 2-Wasserstein distance [18], which is introduced by the gradient structure of dynamics.

In this section, we compare the lower bound of $\langle \sigma \rangle_\tau$ in Eq. (35) with excess EPRs. We focus on the geometric excess EPRs in Refs. [8, 10], since several TSLs that constrain them using the 1-Wasserstein distance have already been discovered. We also compare the TSL in Eq. (35) with the TSL for another distance based on optimal transport theory, i.e., the 2-Wasserstein distance [8, 18].

A. Geometric excess EPRs

We introduce two types of geometric excess EPRs, which are nonnegative lower bounds on the EPR. The first is the *Onsager geometric* excess EPR $\sigma_{\text{ex}}^{\text{ONS}}$ [8], which satisfies $0 \leq \sigma_{\text{ex}}^{\text{ONS}} \leq \sigma$. Based on the form of the EPR in Eq. (30) with $m = L$, this quantity is defined as

$$\sigma_{\text{ex}}^{\text{ONS}} := \min_{J'} \sum_{e \in \mathcal{E}} \frac{J_e'^2}{\mu_{L,e}}. \quad (61)$$

Here, the minimization is performed over all currents J' that reproduces the original time evolution at the moment as

$$d_t x(t) = \nabla^\top J'. \quad (62)$$

Reference [10] provides another definition of the excess EPR, information geometric excess EPR. This is based on the form of the EPR with the KL divergence (12) and defined as

$$\sigma_{\text{ex}}^{\text{IG}} := \min_{J^{+'}, J^{-'}} \{D_{\text{KL}}(J^{+'} \| J^{-}) + D_{\text{KL}}(J^{-'} \| J^{+})\}. \quad (63)$$

Here, the minimization is performed over all fluxes $J^{+'}$ and $J^{-'}$ that reproduces the original time evolution at the moment as

$$d_t x(t) = \nabla^\top (J^{+'} - J^{-'}). \quad (64)$$

This information geometric excess EPR also satisfies $0 \leq \sigma_{\text{ex}}^{\text{IG}} \leq \sigma$. We remark that there is a hierarchy between these two excess EPRs as [10]

$$\sigma_{\text{ex}}^{\text{ONS}} \geq \sigma_{\text{ex}}^{\text{IG}}. \quad (65)$$

B. 2-Wasserstein distance

In Ref. [8], the authors use another Wasserstein distance, that is, the 2-Wasserstein distance, to derive a TSL for the Onsager excess EPR.

Here, we introduce the 2-Wasserstein distance. Since the fluxes depend on x , the activity also depends on x . We write $\mu_{m,e}(x)$ to indicate this dependence on x . If $\mu_{L,e}(x)$ is independent of t , we can define the 2-Wasserstein distance as

$$W_2(x^A, x^B) := \sqrt{\inf_{x', J'} \tau \int_0^\tau dt \sum_{e \in \mathcal{E}} \frac{J_e'^2}{\mu_{L,e}(x')}}}, \quad (66)$$

where x' and J' satisfies

$$x'(0) = x^A, \quad x'(\tau) = x^B, \quad d_t x'(t) = \nabla^\top J'(t). \quad (67)$$

This definition generalizes a formulation of the 2-Wasserstein distance for probability distributions with continuous variables, so called the Benamou–Brenier formula [62]. Equation (66) is introduced for detailed-balanced MJPs in Refs. [18, 52, 53], and extended to more general systems in Ref. [8].

We can measure the speed of the time evolution with the 2-Wasserstein distance as

$$v_2(t) := \lim_{\Delta t \rightarrow 0} \frac{W_2(x(t), x(t + \Delta t))}{\Delta t}. \quad (68)$$

In contrast to the 2-Wasserstein distance itself, we can define this speed even though $\mu_{L,e}(x)$ depends on time, since we can regard $\mu_{L,e}(x)$ as a constant in the infinitesimal time interval. We can relate the speed v_2 to the Onsager geometric excess EPR as

$$\sigma_{\text{ex}}^{\text{ONS}} = v_2^2. \quad (69)$$

This is easily verified as below. Taking $\Delta t \ll 1$, we can reduce the definition of the 2-Wasserstein distance (66) as

$$W_2(x(t), x(t + \Delta t))^2 := \inf_{J'} \Delta t^2 \sum_{e \in \mathcal{E}} \frac{J_e^2}{\mu_{L,e}(x)} + O(\Delta t^3). \quad (70)$$

Here, the conditions (67) make J' satisfy

$$x(t + \Delta t) - x(t) = \Delta t(\nabla^\top J') + O(\Delta t^2). \quad (71)$$

Since this condition is equivalent to Eq. (62) in the limit $\Delta t \rightarrow 0$, we obtain Eq. (69) by dividing the both sides of Eq. (70) and taking the limit $\Delta t \rightarrow 0$.

C. TSLs for geometric excess EPRs

Here, we introduce some TSLs for the geometric excess EPRs and the Wasserstein distances.

The relation in Eq. (69) yields a TSL for the Onsager geometric excess EPR and the 2-Wasserstein distance [8] as

$$\langle \sigma_{\text{ex}}^{\text{ONS}} \rangle_\tau \geq \langle v_2 \rangle_\tau^2. \quad (72)$$

This is easily verified by taking the time integration of Eq. (69) and using the Cauchy–Schwarz inequality as $\int_0^\tau dt \sigma_{\text{ex}}^{\text{ONS}} = \int_0^\tau dt v_2^2 = (\int_0^\tau dt 1^2 \int_0^\tau dt v_2^2) / \tau \geq (\int_0^\tau dt v_2)^2 / \tau$. Since the Onsager geometric excess EPR is smaller than or equivalent to the EPR, we also obtain $\langle \sigma \rangle_\tau \geq \langle v_2 \rangle_\tau^2$. This is a generalization of TSLs for Langevin systems studied in Refs. [3, 6, 63]

We can also obtain the TSL for the Onsager geometric excess EPR and the 1-Wasserstein distance as

$$\langle \sigma_{\text{ex}}^{\text{ONS}} \rangle_\tau \geq \frac{\langle v_1 \rangle_\tau^2}{\langle \mu_L \rangle_\tau}. \quad (73)$$

This is derived for a more general set-up in Ref. [11]. We also provide the proof in Appendix L. We can obtain the TSL [Eq. (35)] for the logarithmic mean $m = L$ by combining Eq. (73) and the inequality $\langle \sigma \rangle_\tau \geq \langle \sigma_{\text{ex}}^{\text{ONS}} \rangle_\tau$.

Reference [10] also provides the TSL for the information geometric excess EPR and the 1-Wasserstein distance as

$$\langle \sigma_{\text{ex}}^{\text{IG}} \rangle_\tau \geq 2 \langle v_1 \rangle_\tau \tanh^{-1} \left(\frac{\langle v_1 \rangle_\tau}{2 \langle \mu_A \rangle_\tau} \right), \quad (74)$$

and thus we can obtain the TSL [Eq. (35)] for the arithmetic mean $m = A$ from the inequality $\langle \sigma \rangle_\tau \geq \langle \sigma_{\text{ex}}^{\text{IG}} \rangle_\tau$. Combining this TSL and the hierarchy in Eq. (65), we also obtain another TSL for the Onsager geometric excess EPR and the 1-Wasserstein distance as

$$\langle \sigma_{\text{ex}}^{\text{ONS}} \rangle_\tau \geq 2 \langle v_1 \rangle_\tau \tanh^{-1} \left(\frac{\langle v_1 \rangle_\tau}{2 \langle \mu_A \rangle_\tau} \right). \quad (75)$$

The above three TSLs can be recast in terms of Ψ_m . The TSLs in Eqs. (73) and (75) imply that $\langle v_1 \rangle_\tau \Psi_m^{-1}(\langle v_1 \rangle_\tau / \langle \mu_m \rangle_\tau)$ becomes a lower bound of the time average of the Onsager geometric excess EPR in the cases

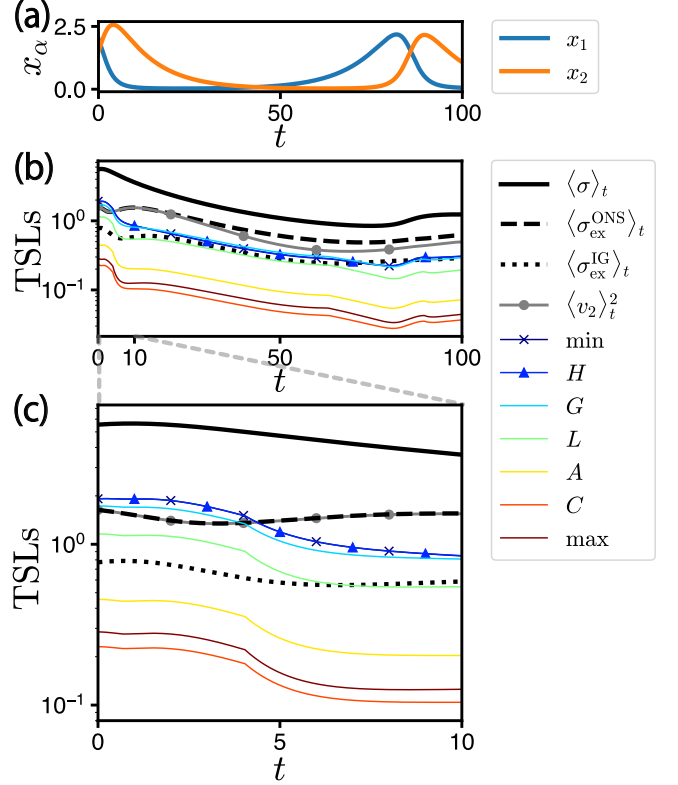


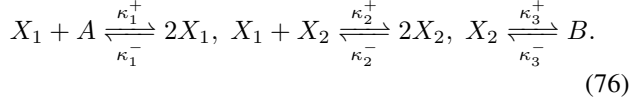
FIG. 2. Comparison of the TSLs [Eq. (35)], the TSL for the 2-Wasserstein distance [Eq. (72)], and the geometric excess EPRs. We use the damped Lotka–Volterra chemical reaction model. (a) The time series of concentration distribution. (b) The TSLs and the geometric excess EPRs. The symbols in the legend indicate the means used to obtain the TSLs, which are the same as those listed in TABLE I. (c) An enlarged view of (b) for the time period $[0, 10]$. Note that the TSLs based on $m = \min$ and $m = H$ overlap as indicated by the markers. The lower bounds $\langle v_1 \rangle_\tau \Psi_m^{-1}(\langle v_1 \rangle_\tau / \langle \mu_m \rangle_\tau)$ for $m = \min, H, G$ can be greater than $\langle \sigma_{\text{ex}}^{\text{IG}} \rangle_\tau$, $\langle \sigma_{\text{ex}}^{\text{ONS}} \rangle_\tau$, and $\langle v_2 \rangle_\tau^2$. In addition, the lower bound for $m = L$ can be greater than $\langle \sigma_{\text{ex}}^{\text{IG}} \rangle_\tau$.

of $m = L$ and $m = A$. The TSL in Eq. (74) implies that $\langle v_1 \rangle_\tau \Psi_m^{-1}(\langle v_1 \rangle_\tau / \langle \mu_m \rangle_\tau)$ becomes a lower bound of the time average of the information geometric excess EPR in the case of $m = A$. Consequently, the TSLs in Eqs. (73), (74), and (75) tighten the lower bound for the total EPR given in Eq. (35) by the excess EPRs.

D. Numerical comparison

Let us consider more deeply the connection between the excess EPRs and general bounds. First, we can ask what if the mean in $\langle v_1 \rangle_\tau \Psi_m^{-1}(\langle v_1 \rangle_\tau / \langle \mu_m \rangle_\tau)$ is not A or L . In addition, it is not certain which is tighter, the TSL (72), which involves the 2-Wasserstein-based speed v_2 , and the TSL (35), containing the 1-Wasserstein speed measure v_1 . In this section, we examine these questions numerically. In particular, we compare the geometric excess EPRs, the TSL for the 2-Wasserstein distance (72), and our TSLs in TABLE II.

Here, we use the following damped Lotka–Volterra chemical reaction model [64]:



Here, we label the reactions as $e = 1, 2,$ and 3 from left to right in Eq. (76). We also assume the mass action kinetics and κ_e^\pm is the reaction rate constant for reaction e . The species A and B are the external ones and their concentrations are fixed as 1. We set the reaction rate constants as $(\kappa_1^+, \kappa_2^+, \kappa_3^+, \kappa_1^-, \kappa_2^-, \kappa_3^-) = (0.1, 0.2, 0.1, 10^{-3}, 10^{-3}, 10^{-5})$. Then, the time evolution of the concentration $x = (x_1, x_2)^\top$ is given by the following rate equation:

$$\begin{cases} d_t x_1 = 0.1x_1 - 10^{-3}x_1^2 - 0.2x_1x_2 + 10^{-3}x_2^2 \\ d_t x_2 = 0.2x_1x_2 - 10^{-3}x_2^2 - 0.1x_2 + 10^{-5} \end{cases}. \quad (77)$$

To demonstrate the TSLs, we use the time series of x obtained by solving the rate equation (77) with the initial condition $x(0) = (2, 1.5)^\top$. This time series is shown in Fig. 2(a).

In Fig. 2(b), we show the comparison of the time-averaged geometric excess EPRs and the lower bounds provided by the TSLs. We can confirm that the TSLs for the geometric excess EPRs in Eqs. (72), (73), (75), and (74) hold. However, the inequality may no longer hold when the combination of the excess EPR and the lower bound (or the mean used) is changed. For example, $\langle v_2 \rangle_\tau^2$ becomes larger than $\langle \sigma_{\text{ex}}^{\text{IG}} \rangle_\tau$ in contrast to Eq. (72). We can also confirm that $\langle v_1 \rangle_\tau \Psi_m^{-1}(\langle v_1 \rangle_\tau / \langle \mu_m \rangle_\tau)$ can exceed the time-averaged excess EPRs for some m . Let us focus on $t \in [0, 10]$ shown in Fig. 2(c). In this period of time, the lower bound $\langle v_1 \rangle_\tau \Psi_m^{-1}(\langle v_1 \rangle_\tau / \langle \mu_m \rangle_\tau)$ for $m = \min, H, G$ can be greater than $\langle \sigma_{\text{ex}}^{\text{IG}} \rangle_\tau$ and $\langle \sigma_{\text{ex}}^{\text{ONS}} \rangle_\tau$. The lower bound $\langle v_1 \rangle_\tau \Psi_L^{-1}(\langle v_1 \rangle_\tau / \langle \mu_L \rangle_\tau)$ also becomes larger than $\langle \sigma_{\text{ex}}^{\text{IG}} \rangle_\tau$. These observations imply that we need to use specific means to bounce geometric excess EPRs.

It is remarkable that some TSLs based on the 1-Wasserstein distance can be tighter than the one based on the 2-Wasserstein distance. In Fig. 2(b), $\langle v_2 \rangle_\tau^2$ becomes larger than the lower bounds based on $\langle v_1 \rangle_\tau$ at most times. However, in Fig. 2(c), the TSLs (35) for $m = \min, H, G$ are possibly tighter than the TSL for the 2-Wasserstein distance. This is different from the case of Langevin systems, where the TSL based on the 1-Wasserstein distance is always weaker than the one based on the 2-Wasserstein distance [11].

VI. DISCUSSION

In this paper, we have derived an infinite variety of TSLs based on the 1-Wasserstein distance. The TSLs can be applied to MJPs and CRNs. We have also related the lower bound of EP provided by each TSL to the minimum dissipation. This minimum dissipation is achievable with a conservative force.

Let us discuss the choice of the mean. As confirmed through numerical calculations, there is no apparent hierarchy among the TSLs. Thus, the mean providing the tightest TSL depends

on the situation. Moreover, the equalities in the TSLs are achievable by minimizing dissipation under the constraint of the time-averaged activity measured with the respective mean. This implies that the previously known TSLs based on the 1-Wasserstein distance [21, 22, 65] are not necessarily the best bounds for the time-averaged EPR.

The choice of the mean becomes crucial for obtaining a lower bound of the time-averaged excess EPRs. This may be because the excess EPRs are defined by optimization problems based on specific means [8, 30]. Therefore, like the TSLs in this work, we may understand the arbitrariness in the definition of excess EPRs [8, 10, 30, 31] from the perspective of means.

Furthermore, it may be possible to characterize an intrinsic lower bound of the time-averaged EPR based on our results. In fact, by selecting the mean that provides the tightest bound at each time, one could obtain a tighter bound than the existing TSLs. The mean that provides the tightest bound may also reflect the characteristics of the dynamics. Hence, it is an interesting challenge to explore the correspondence between the nature of the dynamics and the mean that gives the tightest TSL.

We also discuss the relationship between our results and thermodynamic uncertainty relations (TURs), which describe trade-off relations between the EP and the accuracy [66, 67]. As in the case of TSLs, TURs are also derived in various set-ups using different ways [8, 29, 59, 68–81], and some of them correspond to the means: The arithmetic mean is used to unify the TURs and the TSLs based on the dynamical activity [24, 82–84]. The geometric mean also appears in the initial derivation of TURs [68, 69]. This is because the geometric mean is essential to obtain the rate function, which quantifies fluctuations for the empirical current and distribution [12, 28]. The logarithmic mean is used to derive the TURs for the Onsager geometric excess and housekeeping EPRs [8]. This implies that using a different mean may lead to a different TUR as in the case of the TSLs.

Finally, we introduce some future directions: one direction is to extend our results to open quantum systems. Historically, TSLs for MJPs have been extended to open quantum systems described by the quantum master equation [85, 86]. In particular, reference [22] considers the quantum extension of the second line of the TSLs (35) for $m = A, L$. Reference [87] also develops a quantum version of the relation between force and current in Eq. (26) in the case of $m = L$. Extending the TSLs and the force-current relation to quantum systems with other m remains an open challenge.

The other direction is to elucidate the relationship between our TSLs and classical information-geometric speed limits (ISLs) based on the Fisher information [88–91] and the Cramér-Rao bound [45, 92, 93]. There is a mathematical similarity between the classical ISLs and the TSLs for the 2-Wasserstein distance [6, 11, 61, 94–96]. However, clarifying the similarities and differences between ISLs and the TSLs for the 1-Wasserstein distance is still an open question. Moreover, the classical ISLs originate from the quantum speed limit for quantum systems [97, 98] using the quantum Fisher information [99, 100]. Interestingly, we can define the quantum Fisher information using various means as in the case of the gen-

eral activity [101]. Investigating the connection between our TSLs for classical systems and ISLs for quantum systems [102] would also be an intriguing direction.

ACKNOWLEDGMENTS

Authors thank Artemy Kolchinsky and Naruo Ohga for their suggestive comments. R.N. also thanks Yasushi Okada for their suggestive comments. K.Y. is supported by Grant-in-Aid for JSPS Fellows (Grant No. 22J21619). S.I. is supported by JSPS KAKENHI Grants No. 21H01560, No. 22H01141, No. 23H00467, and No. 24H00834, JST ERATO Grant No. JP-MJER2302, and UTEC-UTokyo FSI Research Grant Program. This research was supported by JSR Fellowship, the University of Tokyo.

Appendix A: The equivalence of the detailed balance condition and the conservativeness

Here we prove the equivalence of the following two statements in the CRN with mass action kinetics and the MJP: (i) the system satisfies the detailed balance condition at time t , and (ii) the forces are conservative at time t .

We only consider the CRN with mass action kinetics, since we can regard the MJP as a special case of the CRN with mass action kinetics. This identification is done by replacing $(n_{\alpha e}^+, n_{\alpha e}^-, \kappa_e^+, \kappa_e^-)$ in the CRN with $(\delta_{\text{as}(e)}, \delta_{\text{at}(e)}, R_{\text{t}(e)\text{s}(e)}^{(r(e))}, R_{\text{s}(e)\text{t}(e)}^{(r(e))})$.

We also remark that the mass action kinetics rewrites the definition of force (9) as

$$\begin{aligned} F_e(t) &= \ln \frac{\kappa_e^+(t) \prod_{\alpha \in \mathcal{S}} [x_\alpha(t)]^{n_{\alpha e}^+}}{\kappa_e^-(t) \prod_{\alpha \in \mathcal{S}} [x_\alpha(t)]^{n_{\alpha e}^-}} \\ &= \ln \frac{\kappa_e^+(t)}{\kappa_e^-(t)} - \sum_{\alpha \in \mathcal{S}} \nabla_{e\alpha} \ln x_\alpha(t). \end{aligned} \quad (\text{A1})$$

First, we prove (i) \Rightarrow (ii). Due to the detailed balance condition, there exist the equilibrium state $x^{\text{eq}}(t)$ that satisfies

$$0 = J_e(x^{\text{eq}}(t), (t)) = J_e^+(x^{\text{eq}}(t), (t)) - J_e^-(x^{\text{eq}}(t), (t)), \quad (\text{A2})$$

for all $e \in \mathcal{E}$. Thus, the equilibrium state satisfies $\ln[J_e^+(x^{\text{eq}}(t), (t))/J_e^-(x^{\text{eq}}(t), (t))] = 0$. The mass action kinetics rewrites this as

$$\begin{aligned} \ln \frac{\kappa_e^+(t)}{\kappa_e^-(t)} &= \ln \frac{\prod_{\alpha \in \mathcal{S}} [x_\alpha^{\text{eq}}(t)]^{n_{\alpha e}^-}}{\prod_{\alpha \in \mathcal{S}} [x_\alpha^{\text{eq}}(t)]^{n_{\alpha e}^+}} \\ &= \sum_{\alpha \in \mathcal{S}} (n_{\alpha e}^- - n_{\alpha e}^+) \ln x_\alpha^{\text{eq}}(t) \\ &= \sum_{\alpha \in \mathcal{S}} \nabla_{e\alpha} \ln x_\alpha^{\text{eq}}(t). \end{aligned} \quad (\text{A3})$$

Combining Eq. (A3) and Eq. (A1), we obtain

$$F_e(t) = - \sum_{\alpha \in \mathcal{S}} \nabla_{e\alpha} \ln \frac{x_\alpha(t)}{x_\alpha^{\text{eq}}(t)}. \quad (\text{A4})$$

We can rewrite this as $F(t) = -\nabla\psi(t)$ using $\psi_\alpha(t) = \ln[x_\alpha(t)/x_\alpha^{\text{eq}}(t)]$. Thus, the forces are conservative at time t .

Second, we prove (ii) \Rightarrow (i). Now, there exists a potential $\psi(t)$ that satisfies $F(t) = -\nabla\psi(t)$. We take $\Xi_\alpha > 0$ arbitrarily so that $\sum_{\alpha \in \mathcal{S}} \nabla_{\alpha e} \ln \Xi_\alpha = 0$ holds for all $e \in \mathcal{E}$. We introduce y using Ξ_α as $y_\alpha := \Xi_\alpha e^{-\psi_\alpha(t) + \ln x_\alpha(t)}$. Then, the state y satisfies $J_e^+(y, t) = J_e^-(y, t)$. This is verified by

$$\begin{aligned} \ln \frac{J_e^+(y, t)}{J_e^-(y, t)} &= \ln \frac{\kappa_e^+(t) \prod_{\alpha \in \mathcal{S}} y_\alpha^{n_{\alpha e}^+}}{\kappa_e^-(t) \prod_{\alpha \in \mathcal{S}} y_\alpha^{n_{\alpha e}^-}} \\ &= \ln \frac{\kappa_e^+(t)}{\kappa_e^-(t)} - \sum_{\alpha \in \mathcal{S}} \nabla_{e\alpha} \ln y_\alpha \\ &= \ln \frac{\kappa_e^+(t)}{\kappa_e^-(t)} - \sum_{\alpha \in \mathcal{S}} \nabla_{e\alpha} \{\ln x_\alpha(t) - \psi_\alpha(t)\} \\ &= F_e(t) + (\nabla\psi(t))_e = 0. \end{aligned} \quad (\text{A5})$$

Here, we use Eq. (A1) in the fourth transform. We note that we can make the values of the conserved quantities [55] in y the same as those in $x(t)$. In particular, we can make y satisfy $\sum_{\alpha \in \mathcal{S}} y_\alpha = 1$ by choosing $\Xi_\alpha = [\sum_{\alpha \in \mathcal{S}} e^{-\psi_\alpha(t) + \ln x_\alpha(t)}]^{-1}$ if we consider the MJP.

Appendix B: The general activity in the continuum limit

We consider a Brownian particle in the n -dimensional Euclidean space. We let $P(\mathbf{r})$ denote the probability density that the particle is located at $\mathbf{r} = (r_i)_{i=1}^n \in \mathbb{R}^n$. We assume that the particle is driven by a potential $V(\mathbf{r})$. We do not assume that the medium is isotropic or homogeneous: the mobility of the i -th direction at \mathbf{r} is given by $\mu_i^{\text{mob}}(\mathbf{r})$ and the temperature at \mathbf{r} is given by $T(\mathbf{r})$. Then, the probability density evolves according to the following Fokker–Planck equation [103]:

$$\begin{aligned} \partial_t P(\mathbf{r}) &= - \sum_{i=1}^n \partial_{r_i} [\mu_i^{\text{mob}}(\mathbf{r}) [\partial_{r_i} V(\mathbf{r})] P(\mathbf{r})] \\ &\quad + \sum_{i=1}^n \partial_{r_i} [\mu_i^{\text{mob}}(\mathbf{r}) \partial_{r_i} [T(\mathbf{r}) P(\mathbf{r})]]. \end{aligned} \quad (\text{B1})$$

We introduce an MJP that discretizes the above system. We consider an n -dimensional square lattice with the lattice constant $\epsilon_L \ll 1$. We let $\alpha = (\alpha_i)_{i=1}^n$ denote the coordinate of a vertex of the lattice. We also define a vector δ^i as

$$(\delta^i)_j := \begin{cases} \epsilon_L & (j = i) \\ 0 & (j \neq i) \end{cases}. \quad (\text{B2})$$

We consider an MJP on this lattice, where the jumps occur only between adjacent vertices. Letting $R_{\alpha \rightarrow \alpha \pm \delta^i}$ denote the

rate of the jump from α to $\alpha \pm \delta^i$, the time evolution of the probability distribution x_α is given by the following linear master equation:

$$d_t x_\alpha = \sum_{i=1}^n (R_{\alpha+\delta^i \rightarrow \alpha} x_{\alpha+\delta^i} - R_{\alpha \rightarrow \alpha+\delta^i} x_\alpha) + \sum_{i=1}^n (R_{\alpha-\delta^i \rightarrow \alpha} x_{\alpha-\delta^i} - R_{\alpha \rightarrow \alpha-\delta^i} x_\alpha). \quad (\text{B3})$$

Here, we define the rate as

$$R_{\alpha \rightarrow \alpha \pm \delta^i} := \frac{\mathcal{A}_i(\alpha)}{\epsilon_L^2} \mp \frac{\mathcal{B}_i(\alpha)}{2\epsilon_L} + O(1), \quad (\text{B4})$$

with

$$\mathcal{A}_i(\alpha) := \mu_i^{\text{mob}}(\alpha) T(\alpha), \quad (\text{B5})$$

$$\mathcal{B}_i(\alpha) := -\mu_i^{\text{mob}}(\alpha) \partial_{r_i} V(\alpha) - T(\alpha) \partial_{r_i} \mu_i^{\text{mob}}(\alpha). \quad (\text{B6})$$

Then, we can rewrite the linear master equation as

$$d_t x_\alpha = \sum_{i=1}^n \left[\frac{\mathcal{B}_i(\alpha + \delta^i) x_{\alpha+\delta^i} - \mathcal{B}_i(\alpha - \delta^i) x_{\alpha-\delta^i}}{2\epsilon_L} \right] + \sum_{i=1}^n \left[\frac{\mathcal{A}_i(\alpha + \delta^i) x_{\alpha+\delta^i} - \mathcal{A}_i(\alpha) x_\alpha}{\epsilon_L^2} - \frac{\mathcal{A}_i(\alpha) x_\alpha - \mathcal{A}_i(\alpha - \delta^i) x_{\alpha-\delta^i}}{\epsilon_L^2} \right] + O(\epsilon_L). \quad (\text{B7})$$

Here, the last term $O(\epsilon_L)$ is derived from the product of $O(1)$ term in the rate (B4) and the difference $x_{\alpha \pm \delta^i} - x_\alpha$. We prove that this MJP recovers the original Fokker–Planck equation (B1) in the continuum limit $\epsilon_L \rightarrow 0$. Note that the probability distribution x_α recovers the probability density $P(r)$ in the continuum limit as

$$P(\alpha) = \lim_{\epsilon_L \rightarrow 0} \frac{x_\alpha}{\epsilon_L^n}. \quad (\text{B8})$$

Due to this fact, we obtain

$$\partial_i P(r) = \sum_{i=1}^n \partial_{r_i} (\mathcal{B}_i(r) P(r)) + \sum_{i=1}^n \partial_{r_i}^2 (\mathcal{A}_i(r) P(r)), \quad (\text{B9})$$

by deviding the both sides of equation (B7) by ϵ_L^n , taking the limit $\epsilon_L \rightarrow 0$, and replacing α with r . Substituting the definition of \mathcal{A}_i and \mathcal{B}_i , we can reduce Eq. (B9) to the original Fokker–Planck equation (B1).

Using this MJP, which converges to the original continuous system, we obtain the following relation,

$$\lim_{\epsilon_L \rightarrow 0} \epsilon_L^2 \mu_m = \int_{\mathbb{R}^n} dr P(r) \sum_{i=1}^n \mu_i^{\text{mob}}(r) T(r), \quad (\text{B10})$$

which indicates the behavior of the general activity in the continuum limit. Due to the Einstein relation, $\mu_i^{\text{mob}}(r) T(r)$

equals the diffusion coefficient for the direction i at r . Thus, the generalized activity corresponds to the average of the diffusion coefficient. Note that this result is invariant for the choice of m .

Let us derive the relation in Eq. (B10). In the MJP, the general activity is given by

$$\mu_m = \frac{1}{2} \sum_{\alpha} \left[\sum_{i=1}^n m (R_{\alpha+\delta^i \rightarrow \alpha} x_{\alpha+\delta^i}, R_{\alpha \rightarrow \alpha+\delta^i} x_\alpha) + \sum_{i=1}^n m (R_{\alpha-\delta^i \rightarrow \alpha} x_{\alpha-\delta^i}, R_{\alpha \rightarrow \alpha-\delta^i} x_\alpha) \right]. \quad (\text{B11})$$

In the following, we explicitly consider the relation Eq. (B8) as $x_\alpha = \epsilon_L^n P(\alpha) + O(\epsilon_L^{n+1})$. We can obtain the asymptotic behavior of $\epsilon_L^2 m (R_{\alpha+\delta^i \rightarrow \alpha} x_{\alpha+\delta^i}, R_{\alpha \rightarrow \alpha+\delta^i} x_\alpha)$ as

$$\begin{aligned} & \epsilon_L^2 m (R_{\alpha+\delta^i \rightarrow \alpha} x_{\alpha+\delta^i}, R_{\alpha \rightarrow \alpha+\delta^i} x_\alpha) \\ &= \epsilon_L^n m (\epsilon_L^2 R_{\alpha+\delta^i \rightarrow \alpha} P(\alpha + \delta^i), \epsilon_L^2 R_{\alpha \rightarrow \alpha+\delta^i} P(\alpha)) \\ &= \epsilon_L^n m (\mathcal{A}_i(\alpha) P(\alpha) + O(\epsilon_L), \mathcal{A}_i(\alpha) P(\alpha) + O(\epsilon_L)) \\ &= \epsilon_L^n \mu_i^{\text{mob}}(\alpha) T(\alpha) P(\alpha) + O(\epsilon_L^{n+1}). \end{aligned} \quad (\text{B12})$$

Here, we use the homogeneity of m in the first transform. In the same manner, we can also obtain

$$\begin{aligned} & \epsilon_L^2 m (R_{\alpha-\delta^i \rightarrow \alpha} x_{\alpha-\delta^i}, R_{\alpha \rightarrow \alpha-\delta^i} x_\alpha) \\ &= \epsilon_L^n \mu_i^{\text{mob}}(\alpha) T(\alpha) P(\alpha) + O(\epsilon_L^{n+1}). \end{aligned} \quad (\text{B13})$$

Combining Eq. (B11) and these asymptotic behaviors, we obtain

$$\begin{aligned} \epsilon_L^2 \mu_m &= \sum_{\alpha} \sum_{i=1}^n [\epsilon_L^n \mu_i^{\text{mob}}(\alpha) T(\alpha) P(\alpha) + O(\epsilon_L^{n+1})] \\ &= \sum_{\alpha} \epsilon_L^n \left[P(\alpha) \sum_{i=1}^n \mu_i^{\text{mob}}(\alpha) T(\alpha) \right] + O(\epsilon_L). \end{aligned} \quad (\text{B14})$$

This equation leads to Eq. (B10) in the continuum limit $\epsilon_L \rightarrow 0$.

Appendix C: Rewriting the two conditions in Eqs. (24) and (25)

In this appendix, we rewrite the conditions on f_m in Eqs. (24) and (25) in terms of the function defined in Eq. (27) as

$$\Psi_m(u) = \frac{e^u - 1}{f_m(e^u)}. \quad (\text{C1})$$

1. Rewriting the first condition (24)

The first condition (24) is equivalent to the monotonically increasingness of Ψ_m . It can be proved as follows: The condition (24) is equivalent to

$$\forall u, f'_m(e^u) + f'_m(e^{-u}) > 0. \quad (\text{C2})$$

This equals the positivity of $\Psi'_m(u)$, since the property of f'_m in Eq. (17) leads to

$$\begin{aligned}\Psi'_m(u) &= \frac{e^u}{f_m(e^u)^2} \{f'_m(e^u) + f_m(e^u) - e^u f'_m(e^u)\} \\ &= \frac{e^u}{f_m(e^u)^2} \{f'_m(e^u) + f'_m(e^{-u})\} > 0.\end{aligned}\quad (\text{C3})$$

Therefore, the first condition lets us define the inverse function Ψ_m^{-1} .

2. Rewriting the second condition (25)

Under the first condition (24), the other condition on f_m (25) is equivalent to the convexity of $w\Psi_m^{-1}(w)$. It can be proved as follows: Since $w\Psi_m^{-1}(w)$ is monotonically increasing on $w > 0$ and even, it is enough to see the convexity of $w\Psi_m^{-1}(w)$ on $w > 0$. Letting u denote $\Psi_m^{-1}(w)$, we obtain

$$(w\Psi_m^{-1}(w))'' = \frac{2\Psi'_m(u)^2 - \Psi_m(u)\Psi''_m(u)}{\Psi'_m(u)^3}, \quad (\text{C4})$$

by direct calculation. Note that the positivity $w > 0$ makes $u = \Psi_m^{-1}(w)$ positive. Since $\Psi'_m(u)$ is positive, the convexity of $w\Psi_m^{-1}(w)$ on $w > 0$ is equivalent to the nonnegativity of the numerator in Eq. (C4) on $u > 0$. We can rewrite the numerator in Eq. (C4) as

$$\begin{aligned}2\Psi'_m(u)^2 - \Psi_m(u)\Psi''_m(u) \\ = \frac{e^u(e^u - 1)^2 f''_m(e^u) + (e^u + 1)(f'_m(e^u) + f'_m(e^{-u}))}{e^{-u} f_m(e^u)^3}.\end{aligned}\quad (\text{C5})$$

Here, we use Eq. (C3),

$$\begin{aligned}e^{-u} f_m(e^u)^3 \Psi''_m(u) \\ = [f_m(e^u) \{(1 - 3e^u)f'_m(e^u) - e^u(e^u - 1)f''_m(e^u)\} \\ + f_m(e^u)^2 + 2e^u(e^u - 1)f'_m(e^u)^2],\end{aligned}\quad (\text{C6})$$

and the relation in Eq. (17). We can verify the equivalence of nonnegativity of Eq. (C5) on $u > 0$ and the condition (25) by taking $r = e^u$. Thus, the condition (25) is equivalent to the convexity of $w\Psi_m^{-1}(w)$.

Appendix D: Availability of various means as the activity

In this appendix, we show that the various means satisfy the conditions in Eqs. (24) and (25). As a preparation, we introduce a useful rewrite of the condition (25),

$$\forall u > 0, \{(\ln \Psi_m(u))'\}^2 - (\ln \Psi_m(u))'' \geq 0. \quad (\text{D1})$$

This expression follows from the fact that the condition (25) is equivalent to $2\Psi'_m(u)^2 - \Psi_m(u)\Psi''_m(u) \geq 0$ for all $u > 0$ as

mentioned in Appendix C2. This representation further leads to Eq. (D1) because

$$\begin{aligned}2\Psi'_m(u)^2 - \Psi_m(u)\Psi''_m(u) \\ = 2 \left(\frac{\Psi'_m(u)}{\Psi_m(u)} \right)^2 \Psi_m(u)^2 - \Psi_m(u) \left(\frac{\Psi'_m(u)}{\Psi_m(u)} \Psi_m(u) \right)' \\ = \Psi_m(u)^2 \left[\left(\frac{\Psi'_m(u)}{\Psi_m(u)} \right)^2 - \left(\frac{\Psi'_m(u)}{\Psi_m(u)} \right)' \right] \\ = \Psi_m(u)^2 \left[\{(\ln \Psi_m(u))'\}^2 - (\ln \Psi_m(u))'' \right].\end{aligned}\quad (\text{D2})$$

1. Stolarsky mean

Here, we verify that the Stolarsky mean (19) satisfies the conditions (24) and (25). The Stolarsky mean satisfies the condition (24) because $S_{p,q}(a, b)$ is monotonically increasing with respect to a and b [104, 105]. We can also prove that the Stolarsky mean satisfies the other condition (25) as below.

Using $S_{p,q}$ as m in Eq. (27), we obtain

$$\Psi_{S_{p,q}}(u) = 2 \sinh \frac{u}{2} \left[\frac{q \sinh(pu/2)}{p \sinh(qu/2)} \right]^{\frac{1}{q-p}}. \quad (\text{D3})$$

Here, we only need to consider the expression in the first line of Eq. (19) due to the continuity of the Stolarsky mean with respect to p and q . This representation yields

$$\begin{aligned}(\ln \Psi_{S_{p,q}}(u))' \\ = \frac{1}{2} \coth \frac{u}{2} - \frac{1}{p-q} \left(\frac{p}{2} \coth \frac{pu}{2} - \frac{q}{2} \coth \frac{qu}{2} \right),\end{aligned}\quad (\text{D4})$$

and

$$\begin{aligned}(\ln \Psi_{S_{p,q}}(u))'' \\ = -\frac{1}{4} \operatorname{csch}^2 \frac{u}{2} + \frac{p^2 \operatorname{csch}^2 \left(\frac{pu}{2} \right) - q^2 \operatorname{csch}^2 \left(\frac{qu}{2} \right)}{4(p-q)},\end{aligned}\quad (\text{D5})$$

which rewrites the left-hand side of Eq. (D1) as

$$\left\{ (\ln \Psi_{S_{p,q}}(u))' \right\}^2 + \frac{1}{4} \operatorname{csch}^2 \frac{u}{2} - \frac{\Theta_1 \left(\frac{pu}{2} \right) - \Theta_1 \left(\frac{qu}{2} \right)}{(p-q)u^2} \quad (\text{D6})$$

with $\Theta_1(z) := z^2 \operatorname{csch}^2 z$, or equivalently,

$$\begin{aligned}\frac{1}{4} \left(\coth^2 \frac{u}{2} + \operatorname{csch}^2 \frac{u}{2} \right) \\ + \left[\frac{1}{p-q} \left(\frac{p}{2} \coth \frac{pu}{2} - \frac{q}{2} \coth \frac{qu}{2} \right) \right]^2 \\ - \frac{\Theta_2 \left(\frac{pu}{2}; \frac{u}{2} \right) - \Theta_2 \left(\frac{qu}{2}; \frac{u}{2} \right)}{(p-q)u^2},\end{aligned}\quad (\text{D7})$$

with $\Theta_2(z; \theta) := z^2 \operatorname{csch}^2 z + (2\theta \coth \theta)z \coth z$. Thus, it is enough to show that one of the following quantities is negative:

$$\left\{ \frac{\Theta_1\left(\frac{pu}{2}\right) - \Theta_1\left(\frac{qu}{2}\right)}{p - q}, \quad (\text{D8}) \right.$$

$$\left. \frac{\Theta_2\left(\frac{pu}{2}; \frac{u}{2}\right) - \Theta_2\left(\frac{qu}{2}; \frac{u}{2}\right)}{p - q}. \quad (\text{D9}) \right.$$

In the following, we only consider $p \geq q$ since the Stolarsky mean is invariant with respect to the swapping of p and q . We can classify $p \geq q$ into the following four cases: (i) $p \geq q \geq 0$, (ii) $p \geq 0 \geq q$ and $p \geq |q|$, (iii) $p \geq 0 \geq q$ and $|q| \geq p$, and (iv) $0 \geq p \geq q$. As shown below, we can prove that Eq. (D8) or Eq. (D9) becomes negative for each case. It concludes that the Stolarsky mean satisfies the condition (25).

In the cases (i) and (ii), we can see that Eq. (D8) is negative because $\Theta_1(z)$ is even and monotonically decreasing on $z \geq 0$. Indeed, this z -dependence of $\Theta_1(z)$ and the nonnegativity of u let $\Theta_1(pu/2) - \Theta_1(qu/2) \leq 0$ hold in these cases. The z -dependence of $\Theta_1(z)$ is verified by using $\coth z \geq 1/z$ on $z \geq 0$ in $\partial_z \Theta_1(z) = -2z^2 \operatorname{csch}^2 z (\coth z - 1/z)$.

In the remaining cases (iii) and (iv), we can see that Eq. (D9) is negative because $\Theta_2(z; \theta)$ is an even function of z and monotonically increasing on $z \geq 0$ for all $\theta > 0$. We can easily see that this z -dependence of $\Theta_2(z; \theta)$ and the nonnegativity of u let $\Theta_2(pu/2; u/2) - \Theta_2(qu/2; u/2) \leq 0$ hold in these cases. The z -dependence of $\Theta_2(z; \theta)$ is verified by the following calculation for $z \geq 0, \theta > 0$,

$$\begin{aligned} \frac{\partial_z \Theta_2(z; \theta)}{2z \operatorname{csch}^2 z} &= 1 - z \coth z + \theta \coth \theta \left(\frac{\sinh 2z}{2z} - 1 \right) \\ &\geq 1 - z \coth z + \left(\frac{\sinh 2z}{2z} - 1 \right) \\ &= \frac{\sinh 2z}{2z} - z \coth z \\ &= \cosh z \left(\frac{\sinh z}{z} - \frac{z}{\sinh z} \right) \\ &\geq 0. \end{aligned} \quad (\text{D10})$$

Here, we use $\theta \coth \theta \geq 1$ on $\theta > 0$ and $(\sinh 2z)/2z \geq 1$ on $z \geq 0$ to derive the first inequality.

2. Contraharmonic mean

Here, we verify that the contraharmonic mean C satisfies the conditions (24) and (25). Using C as m in Eq. (27), we obtain

$$\Psi_C(u) = \tanh u. \quad (\text{D11})$$

It immediately confirms that C satisfies the condition (24), since this condition is equivalent to the monotonic increasingness of Ψ_m as discussed in Appendix C 1. We also obtain

$$(\ln \Psi_C(u))' = \frac{1}{\sinh u \cosh u}, \quad (\text{D12})$$

and

$$(\ln \Psi_C(u))'' = -\frac{1}{\sinh^2 u} - \frac{1}{\cosh^2 u}. \quad (\text{D13})$$

These equations rewrite the left-hand side of Eq. (D1) as $2/\sinh^2 u$, which is nonnegative. Hence the contraharmonic mean also satisfies the conditions (24) and (25).

Appendix E: Legendre duality between current and force

Let us define the dissipation functions [31] as

$$\left\{ \begin{aligned} \Phi_m(F') &:= \sum_{e \in \mathcal{E}} \mu_{m,e} \int_0^{F'_e} du \Psi_m(u), & (\text{E1}) \\ \Phi_m^*(J') &:= \sum_{e \in \mathcal{E}} \mu_{m,e} \int_0^{J'_e/\mu_{m,e}} dw \Psi_m^{-1}(w). & (\text{E2}) \end{aligned} \right.$$

The dissipation functions (E2) are convex since Ψ_m and its inverse are monotonically increasing. They are also related to each other through the Legendre transform. We can verify that the Legendre transform of $\Phi_m^*(J')$ becomes $\Phi_m(F')$ as

$$\begin{aligned} &\sup_{J''} \left\{ \sum_{e \in \mathcal{E}} J''_e F'_e - \Phi_m^*(J'') \right\} \\ &= \sum_{e \in \mathcal{E}} \mu_{m,e} \left\{ F'_e \Psi_m(F'_e) - \int_0^{\Psi_m(F'_e)} dw \Psi_m^{-1}(w) \right\} \\ &= \sum_{e \in \mathcal{E}} \mu_{m,e} \int_0^{F'_e} du \Psi_m(u) = \Phi_m(F'), \end{aligned} \quad (\text{E3})$$

where the second line is obtained from the condition that the J''_e -derivative of the first line vanishes, and the third line is obtained by regarding the first term of the second line as the signed area of $[0, \Psi_m(F'_e)] \times [0, F'_e]$. Using the dissipation functions, we can rewrite the relations between the current and the force as

$$J_e = \partial_{F'_e} \Phi_m(F), \quad F_e = \partial_{J'_e} \Phi_m^*(J). \quad (\text{E4})$$

Historically, the Legendre duality between current and force has been explored in the area of gradient flow [106], which is a branch of mathematics closely related to thermodynamics. First, the linear relation between current and force,

$$J_e = \mu_{L,e} F_e, \quad F_e = \frac{J_e}{\mu_{L,e}}, \quad (\text{E5})$$

is induced by the quadratic dissipation functions,

$$\Phi_L(F') := \frac{1}{2} \sum_{e \in \mathcal{E}} \mu_{L,e} F_e'^2, \quad \Phi_L^*(J') := \frac{1}{2} \sum_{e \in \mathcal{E}} \frac{J_e'^2}{\mu_{L,e}}$$

since $\Psi_L(u) = u$ and $\Psi_L^{-1}(w) = w$. Here, the logarithmic mean L is used as the activity. This result was found for detailed balanced chemical systems [51] and MJPs [18, 52, 53]

as a direct generalization of the works on the Fokker–Planck equation by Otto and his collaborators [107, 108]. This linear relation was extended to more general situations [8, 27] and has been used to reveal the connection between thermodynamics and optimal transport, decompose EPR, and derive thermodynamic trade-off relations [8, 22].

In addition, the nonlinear relation with the geometric mean G being the activity,

$$J_e = 2\mu_{G,e} \sinh\left(\frac{F_e}{2}\right), \quad F_e = 2 \sinh^{-1}\left(\frac{J_e}{2\mu_{G,e}}\right), \quad (\text{E6})$$

corresponding to the nonquadratic dissipation functions,

$$\begin{aligned} \Phi_G(F') &:= 4 \sum_{e \in \mathcal{E}} \mu_{G,e} \left(\cosh \frac{F_e}{2} - 1 \right), \\ \Phi_G^*(J') &:= \sum_{e \in \mathcal{E}} \left[2J_e \sinh^{-1} \frac{J_e}{2\mu_{G,e}} \right. \\ &\quad \left. - 4\mu_{G,e} \left\{ \sqrt{\frac{J_e^2}{4\mu_{G,e}^2} + 1} - 1 \right\} \right], \end{aligned}$$

was discovered by considering the consistency with macroscopic fluctuation theory [25–27]. Here, we used $\Psi_G(u) = 2 \sinh(u/2)$ and $\Psi_G^{-1}(w) = 2 \sinh^{-1}(w/2)$. This nonlinear relation is also used to bound [29] and decompose the EPR [30].

Appendix F: Thermodynamic trade-offs for general currents

1. The derivation of the bound for general currents

The bound (31) is shown as follows. We can obtain a lower bound of the EPR by using the convexity and evenness of the function $w\Psi_m^{-1}(w)$ as

$$\begin{aligned} \sigma &\geq \sum_{e \in \mathcal{E}} \mu_{m,e} \left(\frac{c_e J_e}{|c|_\infty \mu_{m,e}} \right) \Psi_m^{-1} \left(\frac{c_e J_e}{|c|_\infty \mu_{m,e}} \right) \\ &= \sum_{e \in \mathcal{E}} \mu_m \frac{\mu_{m,e}}{\mu_m} \left(\frac{c_e J_e}{|c|_\infty \mu_{m,e}} \right) \Psi_m^{-1} \left(\frac{c_e J_e}{|c|_\infty \mu_{m,e}} \right) \\ &\geq \frac{J_c}{|c|_\infty} \Psi_m^{-1} \left(\frac{J_c}{|c|_\infty \mu_m} \right) \\ &= \frac{|J_c|}{|c|_\infty} \Psi_m^{-1} \left(\frac{|J_c|}{|c|_\infty \mu_m} \right). \end{aligned} \quad (\text{F1})$$

Here, the first line is a consequence of the inequality

$$\frac{J_e}{\mu_{m,e}} \Psi_m^{-1} \left(\frac{J_e}{\mu_{m,e}} \right) \geq \frac{c_e J_e}{|c|_\infty \mu_{m,e}} \Psi_m^{-1} \left(\frac{c_e J_e}{|c|_\infty \mu_{m,e}} \right), \quad (\text{F2})$$

where we use $-1 \leq c_e/|c|_\infty \leq 1$ and the fact that $w\Psi_m^{-1}(w)$ is an even convex function. The inequality between the second and third lines owes to Jensen's inequality with the weight $\{\mu_{m,e}/\mu_m\}_{e \in \mathcal{E}}$. In the last line, we use the evenness of

$w\Psi_m^{-1}(w)$. Taking the time average of Eq. (F1), we obtain the desired result (31)

$$\begin{aligned} \langle \sigma \rangle_\tau &\geq \frac{1}{\tau} \int_0^\tau dt \frac{|J_c|}{|c|_\infty} \Psi_m^{-1} \left(\frac{|J_c|}{|c|_\infty \mu_m} \right) \\ &= \langle \mu_m \rangle_\tau \int_0^\tau dt \frac{\mu_m}{\tau \langle \mu_m \rangle_\tau} \frac{|J_c|}{|c|_\infty \mu_m} \Psi_m^{-1} \left(\frac{|J_c|}{|c|_\infty \mu_m} \right) \\ &\geq \frac{\langle |J_c| \rangle_\tau}{|c|_\infty} \Psi_m^{-1} \left(\frac{\langle |J_c| \rangle_\tau}{|c|_\infty \langle \mu_m \rangle_\tau} \right), \end{aligned} \quad (\text{F3})$$

where we use Jensen's inequality with the weight $\{\mu_m/(\tau \langle \mu_m \rangle_\tau)\}_{t \in [0, \tau]}$ in the last line.

2. Bound for statewise observables

We also introduce the trade-off for the observable $\phi = (\phi_1, \dots, \phi_{N_S})^\top$, which possibly depends on time. This trade-off is a special case of the bound with a general current (31). We use the inner product $\langle x, \varphi \rangle$ between two N_S dimensional vectors x and ϕ , defined as $\langle x, \phi \rangle := \sum_{\alpha \in \mathcal{S}} x_\alpha \phi_\alpha$. In the following, we call the inner product $\langle x, \phi \rangle$ the *expected value* of φ , since it is precisely what is called the expected value in the statistical sense in the case of the MJP.

The trade-off relation is obtained by using the speed of the time evolution measured with the observable ϕ , which is defined as

$$\mathcal{V}_\phi := \langle d_t x, \phi \rangle. \quad (\text{F4})$$

Taking $\nabla \phi$ as c in Eq. (31) and using $\mathcal{J}_{\nabla \phi} = \sum_{e \in \mathcal{E}} (\nabla \phi)_e J_e = \langle \nabla^\top J, \phi \rangle = \langle d_t x, \phi \rangle$, we can easily obtain

$$\langle \sigma \rangle_\tau \geq \frac{\langle |\mathcal{V}_\phi| \rangle_\tau}{|\nabla \phi|_\infty} \Psi_m^{-1} \left(\frac{\langle |\mathcal{V}_\phi| \rangle_\tau}{|\nabla \phi|_\infty \langle \mu_m \rangle_\tau} \right). \quad (\text{F5})$$

Here, we can regard $|\nabla \phi|_\infty$ as the inhomogeneity of the observable on the graph or CRN. This bound (F5) indicates that the larger dissipation required to realize the faster speed measured with the observable ϕ . In contrast to the general case (31), the bound vanishes when the system is in a steady state, since the speed \mathcal{V}_ϕ also vanishes in the steady state.

When the observable ϕ is time independent, the time average of the speed \mathcal{V}_ϕ is bounded by the expected value of ϕ at the initial time 0 and the final time τ as

$$\langle |\mathcal{V}_\phi| \rangle_\tau \geq \langle \mathcal{V}_\phi \rangle_\tau \geq \frac{\langle x(\tau), \phi \rangle - \langle x(0), \phi \rangle}{\tau}, \quad (\text{F6})$$

since the inhomogeneity $|\nabla \phi|_\infty$ is also time independent and the speed \mathcal{V}_ϕ matches the speed of the expected value of ϕ as $\mathcal{V}_\phi = d_t \langle x, \phi \rangle$. The inequality (F6) and the evenness of $w\Psi_m^{-1}(w)$ provide the lower bound of the right hand side in Eq. (F5),

$$\frac{|\langle x(\tau), \phi \rangle - \langle x(0), \phi \rangle|}{\tau |\nabla \phi|_\infty} \Psi_m^{-1} \left(\frac{|\langle x(\tau), \phi \rangle - \langle x(0), \phi \rangle|}{\tau |\nabla \phi|_\infty \langle \mu_m \rangle_\tau} \right), \quad (\text{F7})$$

which is an increasing function of $|\langle x(\tau), \phi \rangle - \langle x(0), \phi \rangle|$ and describes the trade-off between the dissipation and the magnitude of change in the expected value of ϕ over the finite time duration $[0, \tau]$.

Appendix G: Kantorovich–Rubinstein duality

We introduce another representation of the 1-Wasserstein distance, the Kantorovich–Rubinstein duality [17, 20]. In the following part, we use the inner product $\langle \cdot, \cdot \rangle$ introduced in Appendix F 2.

This duality formula is given by the maximization problem

$$W_1(x^A, x^B) = \sup_{\varphi=(\varphi_\alpha)_{\alpha \in \mathcal{S}}} \langle x^B - x^A, \varphi \rangle, \quad (\text{G1})$$

under the condition

$$\max_{e \in \mathcal{E}} |(\nabla \varphi)_e| \leq 1. \quad (\text{G2})$$

The optimizer φ^* of this maximization problem [Eq. (G1)] corresponds to the sign of the optimizer U^* of the Beckmann problem [Eq. (32)]. The relation

$$(\nabla \varphi^*)_e = \frac{U_e^*}{|U_e^*|}, \quad (\text{G3})$$

holds for all $e \in \mathcal{E}^*$, where \mathcal{E}^* is defined as $\mathcal{E}^* := \{e \mid U_e^* \neq 0\}$. This is verified as below. Since the Beckmann problem and the Kantorovich–Rubinstein duality provide the same distance, we obtain

$$\sum_{e \in \mathcal{E}^*} |U_e^*| = \sum_{e \in \mathcal{E}^*} (\nabla \varphi^*)_e U_e^* \quad (\text{G4})$$

by the following calculation: $\sum_{e \in \mathcal{E}^*} |U_e^*| = W_1(x^A, x^B) = \langle x^B - x^A, \varphi^* \rangle = \langle \nabla^\top U^*, \varphi^* \rangle = \sum_{e \in \mathcal{E}^*} (\nabla \varphi^*)_e U_e^*$. The condition in Eq. (G2) also leads to

$$\max_{e \in \mathcal{E}} |(\nabla \varphi^*)_e| \leq 1. \quad (\text{G5})$$

The only way for φ^* to achieve both of Eq. (G4) and Eq. (G5) is to satisfy the desired relation (G3).

Appendix H: Another derivation of the TSLs

In this appendix, we derive the TSLs with the Kantorovich–Rubinstein duality in Appendix G and the trade-off relation for statewise observables in Eq. (F5).

Based on the Kantorovich–Rubinstein duality, the speed measured with the 1-Wasserstein distance v_1 is also given by

$$v_1 = \sup_{\phi=(\phi_\alpha)_{\alpha \in \mathcal{S}}} \langle d_t x, \phi \rangle = \sup_{\phi=(\phi_\alpha)_{\alpha \in \mathcal{S}}} \mathcal{V}_\phi \quad (\text{H1})$$

under the condition

$$\max_{e \in \mathcal{E}} |(\nabla \phi)_e| \leq 1. \quad (\text{H2})$$

Let ϕ^* denote the optimizer of the maximization problem in Eq. (H1). Using ϕ^* as the observable in Eq. (F5), we obtain the TSL (35) as

$$\begin{aligned} \langle \sigma \rangle_\tau &\geq \frac{\langle |\mathcal{V}_{\phi^*}| \rangle_\tau}{|\nabla \phi^*|_\infty} \Psi_m^{-1} \left(\frac{\langle |\mathcal{V}_{\phi^*}| \rangle_\tau}{|\nabla \phi^*|_\infty \langle \mu_m \rangle_\tau} \right) \\ &= \frac{\langle v_1 \rangle_\tau}{|\nabla \phi^*|_\infty} \Psi_m^{-1} \left(\frac{\langle v_1 \rangle_\tau}{|\nabla \phi^*|_\infty \langle \mu_m \rangle_\tau} \right) \\ &= \langle v_1 \rangle_\tau \Psi_m^{-1} \left(\frac{\langle v_1 \rangle_\tau}{\langle \mu_m \rangle_\tau} \right). \end{aligned} \quad (\text{H3})$$

Here, we use $\mathcal{V}_{\phi^*} = v_1$ and $v_1 \geq 0$ between the first and second lines. We also use $|\nabla \phi^*|_\infty = 1$, which follows from the property of the optimizer of the Kantorovich–Rubinstein duality in Eq. (G3).

We remark that the trade-off relation for general observable in Eq. (F5) is looser than the TSL (35). In other words, the following inequality holds for all ϕ :

$$\langle v_1 \rangle_\tau \Psi_m^{-1} \left(\frac{\langle v_1 \rangle_\tau}{\langle \mu_m \rangle_\tau} \right) \geq \frac{\langle |\mathcal{V}_\phi| \rangle_\tau}{|\nabla \phi|_\infty} \Psi_m^{-1} \left(\frac{\langle |\mathcal{V}_\phi| \rangle_\tau}{|\nabla \phi|_\infty \langle \mu_m \rangle_\tau} \right). \quad (\text{H4})$$

We can verify this inequality in the following way. We define a new observable ϕ' as $\phi' := \phi/|\nabla \phi|_\infty$. This new observable satisfies $\mathcal{V}_{\phi'} = \mathcal{V}_\phi/|\nabla \phi|_\infty$. Thus, we can rewrite the right-hand side in Eq. (H4) as

$$\langle |\mathcal{V}_{\phi'}| \rangle_\tau \Psi_m^{-1} \left(\frac{\langle |\mathcal{V}_{\phi'}| \rangle_\tau}{\langle \mu_m \rangle_\tau} \right). \quad (\text{H5})$$

Since the new observable ϕ' satisfies $|\nabla \phi'|_\infty = 1$, the representation of v_1 in Eq. (H1) yields

$$v_1 \geq |\mathcal{V}_{\phi'}|. \quad (\text{H6})$$

We can obtain Eq. (H4) from Eq. (H5) using the inequality (H6) and monotonically increasingness of $\omega \Psi_m^{-1}(\omega)$ on $\omega \geq 0$.

Appendix I: Derivation of the lower bounds of the transition time

Here, we derive the lower bounds of the transition time (44) from the series of TSLs in Eq. (35). From Eq. (35), we obtain

$$\frac{\Sigma_\tau}{l_{1,\tau}} = \frac{\langle \sigma \rangle_\tau}{\langle v_1 \rangle_\tau} \geq \Psi_m^{-1} \left(\frac{\langle v_1 \rangle_\tau}{\langle \mu_m \rangle_\tau} \right) = \Psi_m^{-1} \left(\frac{l_{1,\tau}}{\tau \langle \mu_m \rangle_\tau} \right). \quad (\text{I1})$$

Since $\Psi_m(u)$ increases monotonically on $u \geq 0$, we obtain

$$\Psi_m \left(\frac{\Sigma_\tau}{l_{1,\tau}} \right) \geq \frac{l_{1,\tau}}{\tau \langle \mu_m \rangle_\tau}, \quad (\text{I2})$$

which leads to

$$\frac{\Sigma_\tau}{l_{1,\tau}} \Psi_m \left(\frac{\Sigma_\tau}{l_{1,\tau}} \right) \geq \frac{\Sigma_\tau}{\tau \langle \mu_m \rangle_\tau}. \quad (\text{I3})$$

Considering the monotonically increasingness of $u\Psi_m(u)$ on $u \geq 0$ and the triangle inequality $l_{1,\tau} \geq W_1(x(0), x(\tau))$, we obtain

$$\begin{aligned} & \frac{\Sigma_\tau}{W_1(x(0), x(\tau))} \Psi_m \left(\frac{\Sigma_\tau}{W_1(x(0), x(\tau))} \right) \\ & \geq \frac{\Sigma_\tau}{l_{1,\tau}} \Psi_m \left(\frac{\Sigma_\tau}{l_{1,\tau}} \right) \geq \frac{\Sigma_\tau}{\tau \langle \mu_m \rangle_\tau}. \end{aligned} \quad (\text{I4})$$

Finally, we can derive the desired bounds (44) by dividing this equation by $\Sigma_\tau / \langle \mu_m \rangle_\tau$ and taking the reciprocal.

Appendix J: Weaker TSLs with the total variational distance

The total variation distance,

$$d_{\text{TV}}(x^A, x^B) := \sum_{\alpha \in \mathcal{S}} \frac{|x_\alpha^B - x_\alpha^A|}{2}, \quad (\text{J1})$$

provides a lower bound of the 1-Wasserstein distance as

$$W_1(x^A, x^B) \geq \frac{2d_{\text{TV}}(x^A, x^B)}{M_{|\nabla^\top|}}. \quad (\text{J2})$$

Here, we let $M_{|\nabla^\top|}$ denote $\max_{e \in \mathcal{E}} \sum_{\alpha \in \mathcal{S}} |(\nabla^\top)_{\alpha e}|$, which indicates the maximum value of the number of change in moleculars through one reaction if we consider CRNs. In the case of MJPs, the constant Δ reduces to 2, letting the inequality (J2) be the conventional form $W_1(x^A, x^B) \geq d_{\text{TV}}(x^A, x^B)$. It is verified as $\sum_{\alpha \in \mathcal{S}} |(\nabla^\top)_{\alpha e}| = |(\nabla^\top)_{s(e)e}| + |(\nabla^\top)_{t(e)e}| = |-1| + |1| = 2$ because ∇^\top is an incidence matrix. We can obtain the inequality (J2) using the optimizer of Eq. (32) U^* as

$$\begin{aligned} 2d_{\text{TV}}(x^A, x^B) &= \sum_{\alpha \in \mathcal{S}} \left| \sum_{e \in \mathcal{E}} (\nabla^\top)_{\alpha e} U_e^* \right| \\ &\leq \sum_{e \in \mathcal{E}} \sum_{\alpha \in \mathcal{S}} |(\nabla^\top)_{\alpha e}| |U_e^*| \\ &\leq \left(\max_{e \in \mathcal{E}} \sum_{\alpha \in \mathcal{S}} |(\nabla^\top)_{\alpha e}| \right) \sum_{e \in \mathcal{E}} |U_e^*| \\ &= M_{|\nabla^\top|} W_1(x^A, x^B), \end{aligned} \quad (\text{J3})$$

where we use $x^B - x^A = \nabla^\top U^*$ in the first line.

We can also measure the speed of the time evolution with the total variation distance as

$$v_{\text{TV}} := \lim_{\Delta t \rightarrow 0} \frac{d_{\text{TV}}(x(t), x(t + \Delta t))}{\Delta t} = \frac{1}{2} \sum_{\alpha \in \mathcal{S}} |d_t x_\alpha(t)|. \quad (\text{J4})$$

The inequality between the 1-Wasserstein distance and the total variation distance leads to the inequality between v_1 and v_{TV} ,

$$v_1(t) \geq \frac{2v_{\text{TV}}(t)}{M_{|\nabla^\top|}}. \quad (\text{J5})$$

The inequality between the speeds (J5) and the monotonicity of $\omega\Psi_m^{-1}(\omega)$ leads to the weaker TSL:

$$\begin{aligned} \langle \sigma \rangle_\tau &\geq \langle v_1 \rangle_\tau \Psi_m^{-1} \left(\frac{\langle v_1 \rangle_\tau}{\langle \mu_m \rangle_\tau} \right) \\ &\geq \frac{2\langle v_{\text{TV}} \rangle_\tau}{M_{|\nabla^\top|}} \Psi_m^{-1} \left(\frac{2\langle v_{\text{TV}} \rangle_\tau}{M_{|\nabla^\top|} \langle \mu_m \rangle_\tau} \right). \end{aligned} \quad (\text{J6})$$

Similarly, we obtain

$$\begin{aligned} \langle \sigma \rangle_\tau &\geq \frac{W_1(x(0), x(\tau))}{\tau} \Psi_m^{-1} \left(\frac{W_1(x(0), x(\tau))}{\tau \langle \mu_m \rangle_\tau} \right) \\ &\geq \frac{2d_{\text{TV}}(x(0), x(\tau))}{\tau M_{|\nabla^\top|}} \Psi_m^{-1} \left(\frac{2d_{\text{TV}}(x(0), x(\tau))}{M_{|\nabla^\top|} \langle \mu_m \rangle_\tau} \right), \end{aligned} \quad (\text{J7})$$

using the inequality between the distances (J2). Note that the triangle inequality for the total variation distance leads to

$$\begin{aligned} \langle \sigma \rangle_\tau &\geq \frac{2\langle v_{\text{TV}} \rangle_\tau}{M_{|\nabla^\top|}} \Psi_m^{-1} \left(\frac{2\langle v_{\text{TV}} \rangle_\tau}{M_{|\nabla^\top|} \langle \mu_m \rangle_\tau} \right) \\ &\geq \frac{2d_{\text{TV}}(x(0), x(\tau))}{\tau M_{|\nabla^\top|}} \Psi_m^{-1} \left(\frac{2d_{\text{TV}}(x(0), x(\tau))}{\tau M_{|\nabla^\top|} \langle \mu_m \rangle_\tau} \right). \end{aligned} \quad (\text{J8})$$

Although these bounds are weaker than the one with the 1-Wasserstein distance, they allow us to treat the distribution x and the topology of the graph or the CRNs separately.

Appendix K: Derivation of the minimum dissipation formula based on the Kantorovich–Rubinstein duality

Here, we derive the minimum dissipation formula (58).

First, we prove the inequality

$$\Sigma_\tau[J^+, J^-] \geq W_1(x(0), x(\tau)) \Psi_m^{-1} \left(\frac{W_1(x(0), x(\tau))}{\tau M_0} \right). \quad (\text{K1})$$

Since the TSLs are valid for general time evolution, we obtain

$$\Sigma_\tau[J^+, J^-] \geq W_1(x(0), x(\tau)) \Psi_m^{-1} \left(\frac{W_1(x(0), x(\tau))}{\tau \langle \mu_m \rangle_\tau [J^+, J^-]} \right). \quad (\text{K2})$$

Considering Eq. (57), i.e., $\langle \mu_m \rangle_\tau [J^+, J^-] \leq M_0$ and the monotonically increasingness of $\Psi_m^{-1}(\omega)$ on $\omega \geq 0$, we can obtain the desired inequality.

Second, we construct optimizers J^{+*} and J^{-*} that satisfy the equality of Eq. (K1). Using the optimizers of the Beckmann problem (32) and the Kantorovich–Rubinstein duality (G1), i.e., U^* and φ^* , we define a new potential $\tilde{\varphi}$ as

$$\tilde{\varphi} := -\Psi_m^{-1} \left(\frac{\sum_{e \in \mathcal{E}} |U_e^*|}{\tau M_0} \right) \varphi^*. \quad (\text{K3})$$

With this potential, we define the fluxes J^{+*} and J^{-*} as

$$J_e^{+*} := \begin{cases} \frac{\exp[-(\nabla\tilde{\varphi})_e] U_e^*}{\exp[-(\nabla\tilde{\varphi})_e] - 1} \frac{U_e^*}{\tau} & (e \in \mathcal{E}^*) \\ 0 & (e \in \mathcal{E} \setminus \mathcal{E}^*) \end{cases}, \quad (\text{K4})$$

and

$$J_e^{-*} := \begin{cases} \frac{1}{\exp[-(\nabla\tilde{\varphi})_e] - 1} \frac{U_e^*}{\tau} & (e \in \mathcal{E}^*) \\ 0 & (e \in \mathcal{E} \setminus \mathcal{E}^*) \end{cases}. \quad (\text{K5})$$

Here, we use $\mathcal{E}^* = \{e \mid U_e^* \neq 0\}$ introduced in Appendix G. We can verify that the fluxes satisfy condition (ii) in Eq. (57) as follows. For $e \in \mathcal{E}^*$, we obtain

$$\begin{aligned} m(J_e^{+*}, J_e^{-*}) &= \frac{U_e^* f_m(\exp[-(\nabla\tilde{\varphi})_e])}{\tau \exp[-(\nabla\tilde{\varphi})_e] - 1} \\ &= \frac{U_e^*}{\tau} \frac{1}{\Psi_m(-(\nabla\tilde{\varphi})_e)} \\ &= \frac{U_e^*}{\tau} \left[\Psi_m \left(\Psi_m^{-1} \left(\frac{\sum_{e \in \mathcal{E}} |U_e^*|}{\tau M_0} \right) (\nabla\varphi^*)_e \right) \right]^{-1} \\ &= \frac{U_e^*}{\tau} \left[\Psi_m \left(\Psi_m^{-1} \left(\frac{\sum_{e \in \mathcal{E}} |U_e^*|}{\tau M_0} \right) \frac{U_e^*}{|U_e^*|} \right) \right]^{-1} \\ &= \frac{U_e^*}{\tau} \left[\frac{\sum_{e \in \mathcal{E}} |U_e^*|}{\tau M_0} \frac{U_e^*}{|U_e^*|} \right]^{-1} \\ &= \frac{|U_e^*|}{\sum_{e \in \mathcal{E}^*} |U_e^*|} M_0. \end{aligned} \quad (\text{K6})$$

In the second line, we use the definition of Ψ_m (27). In the fourth line, we use the property of φ^* in Eq. (G3). In the fifth line, we also use the fact that the oddness of Ψ_m leads to $\Psi_m(-\Psi_m^{-1}(\omega)) = -\omega$ for all ω . Finally, we use $\sum_{e \in \mathcal{E}} |U_e^*| = \sum_{e \in \mathcal{E}^*} |U_e^*|$ in the last line. Because $m(J_e^{+*}, J_e^{-*}) = 0$ for all $e \in \mathcal{E} \setminus \mathcal{E}^*$, we obtain

$$\begin{aligned} \langle \mu_m \rangle_\tau [J^{+*}, J^{-*}] &= \frac{1}{\tau} \int_0^\tau dt \sum_{e \in \mathcal{E}} m(J_e^{+*}, J_e^{-*}) \\ &= \frac{1}{\tau} \int_0^\tau dt \sum_{e \in \mathcal{E}^*} \left[\frac{|U_e^*|}{\sum_{e \in \mathcal{E}^*} |U_e^*|} M_0 \right] \\ &= M_0. \end{aligned} \quad (\text{K7})$$

We can also verify that the fluxes J^{+*} and J^{-*} satisfy the

equality of Eq. (K1) as

$$\begin{aligned} \Sigma_\tau [J^{+*}, J^{-*}] &= \int_0^\tau dt \sum_{e \in \mathcal{E}^*} (J_e^{+*} - J_e^{-*}) \ln \frac{J_e^{+*}}{J_e^{-*}} \\ &= \int_0^\tau dt \sum_{e \in \mathcal{E}^*} \frac{U_e^*}{\tau} (-\nabla\tilde{\varphi})_e \\ &= \int_0^\tau dt \sum_{e \in \mathcal{E}^*} \frac{U_e^*}{\tau} \Psi_m^{-1} \left(\frac{\sum_{e \in \mathcal{E}} |U_e^*|}{\tau M_0} \right) (\nabla\varphi^*)_e \\ &= \sum_{e \in \mathcal{E}^*} U_e^* \Psi_m^{-1} \left(\frac{\sum_{e \in \mathcal{E}} |U_e^*|}{\tau M_0} \right) \frac{U_e^*}{|U_e^*|} \\ &= W_1(x(0), x(\tau)) \Psi_m^{-1} \left(\frac{W_1(x(0), x(\tau))}{\tau M_0} \right). \end{aligned} \quad (\text{K8})$$

Here, we use condition (iii), that is, we can regard $(J_e^{+*} - J_e^{-*}) \ln(J_e^{+*}/J_e^{-*}) = 0$ for all $e \in \mathcal{E} \setminus \mathcal{E}^*$, in the first line. We also use the definition of $\tilde{\varphi}$ (K3) in the third line. In the fourth line, we perform the time integration and use the property of φ^* in Eq. (G3). In the last line, we use $\sum_{e \in \mathcal{E}} |U_e^*| = \sum_{e \in \mathcal{E}^*} |U_e^*| = W_1(x(0), x(\tau))$.

We remark some properties of the optimizers J^{+*} and J^{-*} . First, the current $J^* := J^{+*} - J^{-*}$ is independent of time. This is easily verified as

$$J^* = \frac{U^*}{\tau}. \quad (\text{K9})$$

Second, for all e such that $J_e^* \neq 0$, the following equality holds:

$$\ln \frac{J_e^{+*}}{J_e^{-*}} = -(\nabla\tilde{\varphi})_e. \quad (\text{K10})$$

which implies that the optimizers J^{+*} and J^{-*} provide a conservative driving.

Appendix L: Derivation of Eq. (73)

Let J^{ONS} denote the optimizer of the minimization problem in Eq. (61). Due to the condition in Eq. (62), J^{ONS} satisfies $d_t x = \nabla^\top J^{\text{ONS}}$. Thus, we obtain

$$v_1 \leq \sum_{e \in \mathcal{E}} |J_e^{\text{ONS}}| \quad (\text{L1})$$

by the same calculation as for Eq. (34). We can also obtain the following inequality using the Cauchy–Schwarz inequality,

$$\begin{aligned} \mu_L \sigma_{\text{ex}}^{\text{ONS}} &= \left(\sum_{e \in \mathcal{E}} \mu_{L,e} \right) \left\{ \sum_{e \in \mathcal{E}} \frac{(J_e^{\text{ONS}})^2}{\mu_{L,e}} \right\} \\ &= \left(\sum_{e \in \mathcal{E}} \sqrt{\mu_{L,e}^2} \right) \left\{ \sum_{e \in \mathcal{E}} \left(\frac{|J_e^{\text{ONS}}|}{\sqrt{\mu_{L,e}}} \right)^2 \right\} \\ &\geq \left(\sum_{e \in \mathcal{E}} |J_e^{\text{ONS}}| \right)^2. \end{aligned} \quad (\text{L2})$$

These two inequalities in Eqs. (L1) and (L2) yield

$$v_1 \leq \sqrt{\mu_L \sigma_{\text{ex}}^{\text{ONS}}}. \quad (\text{L3})$$

Integrating both sides of this inequality, we obtain

$$\begin{aligned} \tau \langle v_1 \rangle_\tau &\leq \int_0^\tau dt \sqrt{\mu_L \sigma_{\text{ex}}^{\text{ONS}}} \\ &\leq \sqrt{\int_0^\tau dt \mu_L} \sqrt{\int_0^\tau dt \sigma_{\text{ex}}^{\text{ONS}}} \\ &= \tau \sqrt{\langle \mu_L \rangle_\tau \langle \sigma_{\text{ex}}^{\text{ONS}} \rangle_\tau}. \end{aligned} \quad (\text{L4})$$

Here, the second inequality follows from the Cauchy–Schwarz inequality. The inequality in Eq. (L4) implies $\langle v_1 \rangle_\tau^2 \leq \langle \mu_L \rangle_\tau \langle \sigma_{\text{ex}}^{\text{ONS}} \rangle_\tau$, which equals the desired TSL in Eq. (73).

-
- [1] K. Sekimoto, *Stochastic Energetics* (Springer Berlin Heidelberg, 2010).
- [2] U. Seifert, Stochastic thermodynamics, fluctuation theorems and molecular machines, *Reports on progress in physics* **75**, 126001 (2012).
- [3] E. Aurell, K. Gawędzki, C. Mejía-Monasterio, R. Mohayae, and P. Muratore-Ginanneschi, Refined second law of thermodynamics for fast random processes, *Journal of statistical physics* **147**, 487 (2012).
- [4] N. Shiraishi, K. Funo, and K. Saito, Speed limit for classical stochastic processes, *Physical review letters* **121**, 070601 (2018).
- [5] Y. Chen, T. T. Georgiou, and A. Tannenbaum, Stochastic control and nonequilibrium thermodynamics: Fundamental limits, *IEEE transactions on automatic control* **65**, 2979 (2019).
- [6] M. Nakazato and S. Ito, Geometrical aspects of entropy production in stochastic thermodynamics based on wasserstein distance, *Physical Review Research* **3**, 043093 (2021).
- [7] K. Yoshimura and S. Ito, Thermodynamic uncertainty relation and thermodynamic speed limit in deterministic chemical reaction networks, *Physical review letters* **127**, 160601 (2021).
- [8] K. Yoshimura, A. Kolchinsky, A. Dechant, and S. Ito, House-keeping and excess entropy production for general nonlinear dynamics, *Physical Review Research* **5**, 013017 (2023).
- [9] T. Van Vu and K. Saito, Topological speed limit, *Physical review letters* **130**, 010402 (2023).
- [10] A. Kolchinsky, A. Dechant, K. Yoshimura, and S. Ito, Generalized free energy and excess entropy production for active systems, *arXiv preprint arXiv:2412.08432* (2024).
- [11] R. Nagayama, K. Yoshimura, A. Kolchinsky, and S. Ito, Geometric thermodynamics of reaction-diffusion systems: Thermodynamic trade-off relations and optimal transport for pattern formation, *arXiv preprint arXiv:2311.16569* (2023).
- [12] C. Maes and K. Netočný, Canonical structure of dynamical fluctuations in mesoscopic nonequilibrium steady states, *EPL (Europhysics Letters)* **82**, 30003 (2008).
- [13] J. S. Lee, S. Lee, H. Kwon, and H. Park, Speed limit for a highly irreversible process and tight finite-time landauer’s bound, *Physical review letters* **129**, 120603 (2022).
- [14] T. Van Vu, Y. Hasegawa, *et al.*, Unified thermodynamic–kinetic uncertainty relation, *Journal of Physics A: Mathematical and Theoretical* **55**, 405004 (2022).
- [15] G. Falasco, M. Esposito, and J.-C. Delvenne, Beyond thermodynamic uncertainty relations: nonlinear response, error-dissipation trade-offs, and speed limits, *Journal of Physics A: Mathematical and Theoretical* **55**, 124002 (2022).
- [16] J.-C. Delvenne and G. Falasco, Thermokinetic relations, *Physical Review E* **109**, 014109 (2024).
- [17] C. Villani *et al.*, *Optimal transport: old and new*, Vol. 338 (Springer, 2009).
- [18] J. Maas, Gradient flows of the entropy for finite markov chains, *Journal of Functional Analysis* **261**, 2250 (2011).
- [19] F. Santambrogio, Optimal transport for applied mathematicians, *Birkhäuser, NY* **55**, 94 (2015).
- [20] G. Peyré, M. Cuturi, *et al.*, Computational optimal transport: With applications to data science, *Foundations and Trends® in Machine Learning* **11**, 355 (2019).
- [21] A. Dechant, Minimum entropy production, detailed balance and wasserstein distance for continuous-time markov processes, *Journal of Physics A: Mathematical and Theoretical* **55**, 094001 (2022).
- [22] T. Van Vu and K. Saito, Thermodynamic unification of optimal transport: thermodynamic uncertainty relation, minimum dissipation, and thermodynamic speed limits, *Physical Review X* **13**, 011013 (2023).
- [23] T. Hatano and S.-i. Sasa, Steady-state thermodynamics of langevin systems, *Physical review letters* **86**, 3463 (2001).
- [24] V. T. Vo, T. Van Vu, and Y. Hasegawa, Unified approach to classical speed limit and thermodynamic uncertainty relation, *Physical Review E* **102**, 062132 (2020).
- [25] A. Mielke, M. A. Peletier, and D. M. Renger, On the relation between gradient flows and the large-deviation principle, with applications to markov chains and diffusion, *Potential Analysis* **41**, 1293 (2014).
- [26] A. Mielke, R. I. Patterson, M. A. Peletier, and D. Michiel Renger, Non-equilibrium thermodynamical principles for chemical reactions with mass-action kinetics, *SIAM Journal on Applied Mathematics* **77**, 1562 (2017).
- [27] M. Kaiser, R. L. Jack, and J. Zimmer, Canonical structure and orthogonality of forces and currents in irreversible markov chains, *Journal of Statistical Physics* **170**, 1019 (2018).
- [28] A. C. Barato and R. Chetrite, A formal view on level 2.5 large deviations and fluctuation relations, *Journal of Statistical Physics* **160**, 1154–1172 (2015).
- [29] C. Maes, Frenetic bounds on the entropy production, *Physical review letters* **119**, 160601 (2017).
- [30] T. J. Kobayashi, D. Loutchko, A. Kamimura, and Y. Sughiyama, Hessian geometry of nonequilibrium chemical reaction networks and entropy production decompositions, *Physical Review Research* **4**, 033208 (2022).

- [31] T. J. Kobayashi, D. Loutchko, A. Kamimura, S. A. Horiguchi, and Y. Sughiyama, Information geometry of dynamics on graphs and hypergraphs, *Information Geometry*, **1** (2023).
- [32] M. A. Peletier, R. Rossi, G. Savaré, and O. Tse, Jump processes as generalized gradient flows, *Calculus of Variations and Partial Differential Equations* **61**, 1 (2022).
- [33] K. B. Stolarsky, Generalizations of the logarithmic mean, *Mathematics Magazine* **48**, 87 (1975).
- [34] R. Cisbani, Contributi alla teoria delle medie, *METRON* **13**, 23 (1938).
- [35] M. Tobey, A two-parameter homogeneous mean value, *Proceedings of the American Mathematical Society* **18**, 9 (1967).
- [36] B. Remlein and U. Seifert, Optimality of nonconservative driving for finite-time processes with discrete states, *Physical Review E* **103**, L050105 (2021).
- [37] E. Ilker, Ö. Güngör, B. Kuznets-Speck, J. Chiel, S. Deffner, and M. Hinczewski, Shortcuts in stochastic systems and control of biophysical processes, *Physical Review X* **12**, 021048 (2022).
- [38] H. Ge and H. Qian, Mesoscopic kinetic basis of macroscopic chemical thermodynamics: A mathematical theory, *Physical Review E* **94**, 052150 (2016).
- [39] R. Rao and M. Esposito, Nonequilibrium thermodynamics of chemical reaction networks: Wisdom from stochastic thermodynamics, *Physical Review X* **6**, 041064 (2016).
- [40] J. A. Bondy and U. S. R. Murty, *Graph theory* (Springer Publishing Company, Incorporated, 2008).
- [41] M. Feinberg, Foundations of chemical reaction network theory, *Applied Mathematical Sciences* **10.1007/978-3-030-03858-8** (2019).
- [42] D. Kondepudi and I. Prigogine, *Modern thermodynamics: from heat engines to dissipative structures* (John Wiley & sons, 2014).
- [43] D. A. Beard and H. Qian, Relationship between thermodynamic driving force and one-way fluxes in reversible processes, *PLoS one* **2**, e144 (2007).
- [44] C. Maes, Local detailed balance, *SciPost Physics Lecture Notes*, 032 (2021).
- [45] K. Yoshimura and S. Ito, Information geometric inequalities of chemical thermodynamics, *Physical Review Research* **3**, 013175 (2021).
- [46] S. Schuster and R. Schuster, A generalization of Wegscheider's condition. implications for properties of steady states and for quasi-steady-state approximation, *Journal of Mathematical Chemistry* **3**, 25 (1989).
- [47] F. Kubo and T. Ando, Means of positive linear operators, *Mathematische Annalen* **246**, 205 (1980).
- [48] Á. Besenyei, The hasegawa–petz mean: properties and inequalities, *Journal of Mathematical Analysis and Applications* **391**, 441 (2012).
- [49] P. S. Bullen, *Handbook of means and their inequalities*, Vol. 560 (Springer Science & Business Media, 2013).
- [50] L. Galvani, Dei limiti a cui tendono alcune medie, *Bollettino dell'Unione Matematica Italiana* **1**, 6, 173 (1927).
- [51] A. Mielke, A gradient structure for reaction–diffusion systems and for energy-drift-diffusion systems, *Nonlinearity* **24**, 1329 (2011).
- [52] S.-N. Chow, W. Huang, Y. Li, and H. Zhou, Fokker–planck equations for a free energy functional or markov process on a graph, *Archive for Rational Mechanics and Analysis* **203**, 969 (2012).
- [53] A. Mielke, Geodesic convexity of the relative entropy in reversible markov chains, *Calculus of Variations and Partial Differential Equations* **48**, 1 (2013).
- [54] M. Beckmann, A continuous model of transportation, *Econometrica: Journal of the Econometric Society*, 643 (1952).
- [55] J. Schnakenberg, Network theory of microscopic and macroscopic behavior of master equation systems, *Reviews of Modern physics* **48**, 571 (1976).
- [56] Y. Oono and M. Paniconi, Steady state thermodynamics, *Progress of Theoretical Physics Supplement* **130**, 29 (1998).
- [57] C. Maes and K. Netočný, A nonequilibrium extension of the clausius heat theorem, *Journal of Statistical Physics* **154**, 188 (2014).
- [58] M. Esposito and C. Van den Broeck, Three faces of the second law. i. master equation formulation, *Physical Review E—Statistical, Nonlinear, and Soft Matter Physics* **82**, 011143 (2010).
- [59] A. Dechant, S.-i. Sasa, and S. Ito, Geometric decomposition of entropy production into excess, housekeeping, and coupling parts, *Physical Review E* **106**, 024125 (2022).
- [60] A. Dechant, S.-i. Sasa, and S. Ito, Geometric decomposition of entropy production in out-of-equilibrium systems, *Physical Review Research* **4**, L012034 (2022).
- [61] S. Ito, Geometric thermodynamics for the fokker–planck equation: stochastic thermodynamic links between information geometry and optimal transport, *Information Geometry* **7**, 441 (2024).
- [62] J.-D. Benamou and Y. Brenier, A computational fluid mechanics solution to the monge-kantorovich mass transfer problem, *Numerische Mathematik* **84**, 375 (2000).
- [63] E. Aurell, C. Mejía-Monasterio, and P. Muratore-Ginanneschi, Optimal protocols and optimal transport in stochastic thermodynamics, *Physical review letters* **106**, 250601 (2011).
- [64] S. H. Strogatz, *Nonlinear dynamics and chaos: with applications to physics, biology, chemistry, and engineering* (CRC press, 2018).
- [65] R. Nagase and T. Sagawa, Thermodynamically optimal information gain in finite-time measurement, *Physical Review Research* **6**, 033239 (2024).
- [66] A. C. Barato and U. Seifert, Thermodynamic uncertainty relation for biomolecular processes, *Physical review letters* **114**, 158101 (2015).
- [67] J. M. Horowitz and T. R. Gingrich, Thermodynamic uncertainty relations constrain non-equilibrium fluctuations, *Nature Physics* **16**, 15 (2020).
- [68] T. R. Gingrich, J. M. Horowitz, N. Perunov, and J. L. England, Dissipation bounds all steady-state current fluctuations, *Physical Review Letters* **116**, 10.1103/physrevlett.116.120601 (2016).
- [69] J. M. Horowitz and T. R. Gingrich, Proof of the finite-time thermodynamic uncertainty relation for steady-state currents, *Physical Review E* **96**, 020103 (2017).
- [70] K. Proesmans and C. Van den Broeck, Discrete-time thermodynamic uncertainty relation, *Europhysics Letters* **119**, 20001 (2017).
- [71] P. Pietzonka, F. Ritort, and U. Seifert, Finite-time generalization of the thermodynamic uncertainty relation, *Physical Review E* **96**, 10.1103/physreve.96.012101 (2017).
- [72] A. Dechant and S.-i. Sasa, Current fluctuations and transport efficiency for general langevin systems, *Journal of Statistical Mechanics: Theory and Experiment* **2018**, 063209 (2018).
- [73] A. Dechant, Multidimensional thermodynamic uncertainty relations, *Journal of Physics A: Mathematical and Theoretical* **52**, 035001 (2018).
- [74] A. M. Timpanaro, G. Guarnieri, J. Goold, and G. T. Landi, Thermodynamic uncertainty relations from exchange fluctuation theorems, *Physical Review Letters* **123**, 10.1103/phys-

- revlett.123.090604 (2019).
- [75] P. P. Potts and P. Samuelsson, Thermodynamic uncertainty relations including measurement and feedback, *Physical Review E* **100**, 052137 (2019).
- [76] Y. Hasegawa and T. Van Vu, Fluctuation theorem uncertainty relation, *Physical Review Letters* **123**, 10.1103/physrevlett.123.110602 (2019).
- [77] A. Dechant and S.-i. Sasa, Improving thermodynamic bounds using correlations, *Physical Review X* **11**, 10.1103/physrevx.11.041061 (2021).
- [78] A. Dechant and S.-i. Sasa, Fluctuation–response inequality out of equilibrium, *Proceedings of the National Academy of Sciences* **117**, 6430–6436 (2020).
- [79] S. Otsubo, S. Ito, A. Dechant, and T. Sagawa, Estimating entropy production by machine learning of short-time fluctuating currents, *Physical Review E* **101**, 062106 (2020).
- [80] K. Liu, Z. Gong, and M. Ueda, Thermodynamic uncertainty relation for arbitrary initial states, *Physical Review Letters* **125**, 10.1103/physrevlett.125.140602 (2020).
- [81] E. Kwon, J.-M. Park, J. S. Lee, and Y. Baek, Unified hierarchical relationship between thermodynamic tradeoff relations, *Physical Review E* **110**, 044131 (2024).
- [82] G. Falasco, M. Esposito, and J.-C. Delvenne, Unifying thermodynamic uncertainty relations, *New Journal of Physics* **22**, 053046 (2020).
- [83] V. T. Vo, T. Van Vu, and Y. Hasegawa, Unified thermodynamic–kinetic uncertainty relation, *Journal of Physics A: Mathematical and Theoretical* **55**, 405004 (2022).
- [84] Y. Hasegawa, Unifying speed limit, thermodynamic uncertainty relation and heisenberg principle via bulk-boundary correspondence, *Nature Communications* **14**, 10.1038/s41467-023-38074-8 (2023).
- [85] K. Funo, N. Shiraishi, and K. Saito, Speed limit for open quantum systems, *New Journal of Physics* **21**, 013006 (2019).
- [86] T. Van Vu and Y. Hasegawa, Geometrical bounds of the irreversibility in markovian systems, *Physical Review Letters* **126**, 010601 (2021).
- [87] K. Yoshimura, Y. Maekawa, R. Nagayama, and S. Ito, Force-current structure in markovian open quantum systems and its applications: geometric housekeeping-excess decomposition and thermodynamic trade-off relations, *arXiv preprint arXiv:2410.22628* (2024).
- [88] P. Salamon and R. S. Berry, Thermodynamic length and dissipated availability, *Physical Review Letters* **51**, 1127 (1983).
- [89] G. E. Crooks, Measuring thermodynamic length, *Physical Review Letters* **99**, 100602 (2007).
- [90] D. A. Sivak and G. E. Crooks, Thermodynamic metrics and optimal paths, *Physical review letters* **108**, 190602 (2012).
- [91] S. Ito, Stochastic thermodynamic interpretation of information geometry, *Physical review letters* **121**, 030605 (2018).
- [92] S. Ito and A. Dechant, Stochastic time evolution, information geometry, and the cramér-rao bound, *Physical Review X* **10**, 021056 (2020).
- [93] S. B. Nicholson, L. P. García-Pintos, A. del Campo, and J. R. Green, Time–information uncertainty relations in thermodynamics, *Nature Physics* **16**, 1211 (2020).
- [94] W. Li and J. Zhao, Wasserstein information matrix, *Information Geometry* **6**, 203 (2023).
- [95] S. Chennakesavalu and G. M. Rotskoff, Unified, geometric framework for nonequilibrium protocol optimization, *Physical Review Letters* **130**, 107101 (2023).
- [96] A. Zhong and M. R. DeWeese, Beyond linear response: Equivalence between thermodynamic geometry and optimal transport, *Physical Review Letters* **133**, 057102 (2024).
- [97] L. Mandelstam and I. Tamm, The uncertainty relation between energy and time in non-relativistic quantum mechanics, in *Selected papers* (Springer, 1991) pp. 115–123.
- [98] J. Anandan and Y. Aharonov, Geometry of quantum evolution, *Physical review letters* **65**, 1697 (1990).
- [99] D. P. Pires, M. Cianciaruso, L. C. Céleri, G. Adesso, and D. O. Soares-Pinto, Generalized geometric quantum speed limits, *Physical Review X* **6**, 021031 (2016).
- [100] L. P. García-Pintos, S. B. Nicholson, J. R. Green, A. del Campo, and A. V. Gorshkov, Unifying quantum and classical speed limits on observables, *Physical Review X* **12**, 10.1103/physrevx.12.011038 (2022).
- [101] D. Petz and C. Ghinea, Introduction to quantum fisher information, in *Quantum probability and related topics* (World Scientific, 2011) pp. 261–281.
- [102] L. P. Bettmann and J. Goold, Information geometry approach to quantum stochastic thermodynamics, *arXiv preprint arXiv:2409.06083* (2024).
- [103] N. Van Kampen, Diffusion in inhomogeneous media, *Journal of physics and chemistry of solids* **49**, 673 (1988).
- [104] E. B. Leach and M. C. Sholander, Extended mean values, *The American Mathematical Monthly* **85**, 84 (1978).
- [105] E. Leach and M. Sholander, Extended mean values ii, *Journal of Mathematical Analysis and Applications* **92**, 207 (1983).
- [106] L. Ambrosio, N. Gigli, and G. Savaré, *Gradient flows: in metric spaces and in the space of probability measures* (Springer Science & Business Media, 2005).
- [107] R. Jordan, D. Kinderlehrer, and F. Otto, The variational formulation of the fokker–planck equation, *SIAM journal on mathematical analysis* **29**, 1 (1998).
- [108] F. Otto, The geometry of dissipative evolution equations: the porous medium equation, *Communications in Partial Differential Equations* **26**, 101 (2001).